UNIVERSIDADE FEDERAL DE VIÇOSA

Padrões espaço-temporais de transporte de água atmosférica e umidade do solo na América do Sul de 1980 a 2020

Youlia Kamei Saito
Doctor Scientiae

VIÇOSA - MINAS GERAIS
2025

YOULIA KAMEI SAITO

Padrões espaço-temporais de transporte de água atmosférica e umidade do solo na América do Sul de 1980 a 2020

Tese apresentada à Universidade Federal de Viçosa, como parte das exigências do Programa de Pós-Graduação em Meteorologia Aplicada, para obtenção do título de *Doctor Scientiae*.

Orientador: Flavio Barbosa Justino

Coorientador: Carlos D. de Sousa Gurjão

VIÇOSA - MINAS GERAIS
2025

Ficha catalográfica elaborada pela Biblioteca Central da Universidade Federal de Viçosa - Campus Viçosa

T
S158s
2025

Saito, Youlia Kamei, 1993-
Padrões espaço-temporais de transporte de água atmosférica e umidade do solo na América do Sul de 1980 a 2020 / Youlia Kamei Saito. – Viçosa, MG, 2025.
1 tese eletrônica (94 f.): il. (algumas color.).

Texto em português e inglês.
Orientador: Flávio Barbosa Justino.
Tese (doutorado) - Universidade Federal de Viçosa, Departamento de Engenharia Agrícola, 2025.
Inclui bibliografia.
DOI: https://doi.org/10.47328/ufvbbt.2025.635
Modo de acesso: World Wide Web.

1. Balanço hidrológico - América do Sul. 2. Interação oceano-atmosfera - América do Sul. 3. Solos - Umidade. 4. Incêndios florestais - Previsão. 5. Clima - Brasil. 6. Cerrados. I. Justino, Flávio Barbosa, 1971-. II. Universidade Federal de Viçosa. Departamento de Engenharia Agrícola. Programa de Pós-Graduação em Meteorologia Aplicada. III. Título.

CDD 22. ed. 551.48

Bibliotecário(a) responsável: Euzébio Luiz Pinto CRB-6/3317

YOULIA KAMEI SAITO

Padrões espaço-temporais de transporte de água atmosférica e umidade do solo na América do Sul de 1980 a 2020

Tese apresentada à Universidade Federal de Viçosa, como parte das exigências do Programa de Pós-Graduação em Meteorologia Aplicada, para obtenção do título de *Doctor Scientiae*.

APROVADA: 7 de março de 2025.

Assentimento:

_____

Youlia Kamei Saito
Autora

_____

Flavio Barbosa Justino
Orientador

Essa tese foi assinada digitalmente pela autora em 09/10/2025 às 11:40:08 e pelo orientador em 09/10/2025 às 14:51:51. As assinaturas têm validade legal, conforme o disposto na Medida Provisória 2.200-2/2001 e na Resolução nº 37/2012 do CONARQ. Para conferir a autenticidade, acesse https://siadoc.ufv.br/validar-documento. No campo 'Código de registro', informe o código **GEFQ.YHGY.C2NE** e clique no botão 'Validar documento'.

To God and to my family.

AGRADECIMENTOS

Gostaria de expressar minha mais profunda gratidão aos meus pais, Mitie e Norton, pelo amor incondicional, incentivo e apoio inabalável ao longo da minha vida.
Ao meu marido, Arthur, por seu amor, riso, paciência e constante apoio em cada momento desta jornada.
A toda a minha família — Batchan, tios e primos — que sempre estiveram ao meu lado, torcendo por mim e me encorajando a perseguir meus sonhos.
À minha família de quatro patas, Nenem, Miucha e Cottage, que me fizeram companhia em incontáveis aulas, horas de pesquisa e análises de dados.
Ao Professor Flavio Justino, pela orientação inestimável ao longo dos anos e por sempre me inspirar a buscar novos conhecimentos.
Ao Carlos Gurjão, pelo apoio fundamental durante todos esses anos, sempre oferecendo ajuda generosa sempre que precisei. Meus sinceros agradecimentos também a todos os meus colegas da Meteorologia: Pedro Thiago, Pedro Arthur, Ícaro, Leticia, Aninha, Bruna, Lormido, Elaine, Thais e Santiago.
À Professora Francina Dominguez, da Universidade de Illinois em Urbana-Champaign, por suas valiosas sugestões e apoio durante meu intercâmbio de doutorado.
Ao SeungUk Kim, por sua generosa ajuda na realização deste projeto. E ao Grupo de Hidrometeorologia pelo apoio.
Às minhas amigas de infância, Mariane, Bia e Poliana, pelo carinho e incentivo em todas as fases da vida.
Aos meus amigos da UFV — Pedro, Lucas, Hilda, Natália, Lara, Débora, Bárbara, Iann, Kamila, Fernanda, Priscila, Larissa, Erick, Marconi, Guilherme ... — obrigada pela amizade e encorajamento durante esta jornada.
Aos meus amigos de Bristol, Sapporo e Urbana-Champaign — Vania, Heloisa, Marcella, Flat 407, Andressa, Flavio, Diana, Ayumi, Patricia, Julia, Lindomar, Isadora, Filipe, Roberta, Gabriela, Jairo, Paula, Elis, Thais, João, Thallyta, Lucas — que fizeram com que cada lugar do mundo parecesse um lar.
A todos os professores que cruzaram meu caminho, pelo conhecimento compartilhado e pela dedicação ao ensino.
À Graça Freitas, que sempre nos incentivou e que torna o programa de Meteorologia Aplicada mais prazeroso.
À Universidade Federal de Viçosa, pela oportunidade de concluir meus

estudos de pós-graduação e por oferecer uma educação de excelência desde a graduação.
Este trabalho foi realizado com o apoio das seguintes agências de pesquisa brasileiras: Coordenação de Aperfeiçoamento de Pessoal de Nível Superior – Brasil (CAPES) – Código de Financiamento 001, Fundação de Amparo à Pesquisa do Estado de Minas Gerais (FAPEMIG) e Conselho Nacional de Desenvolvimento Científico e Tecnológico (CNPq).

“The world is a fine place and worth fighting for.”
(Ernest Hemingway)

RESUMO

SAITO, Youlia Kamei, D.Sc., Universidade Federal de Viçosa, março de 2025. **Padrões espaço-temporais de transporte de água atmosférica e umidade do solo na América do Sul de 1980 a 2020**. Orientador: Flavio Barbosa Justino. Coorientador: Carlos Diego de Sousa Gurjão.

A região do Cerrado no Brasil é uma zona ecológica e agrícola crucial, significativamente influenciada pelos fluxos atmosféricos de umidade que regulam a precipitação, a umidade do solo e a atividade de incêndios. Este estudo analisa as interações entre a variabilidade da umidade do solo, o transporte atmosférico de umidade e a dinâmica do fogo, considerando os principais fatores climáticos em grande escala, como o El Niño-Oscilação Sul (ENSO) e a Variabilidade Tropical do Atlântico (TAV). O aporte de umidade dos oceanos Atlântico e Pacífico, bem como da Bacia Amazônica, desempenha um papel fundamental no equilíbrio hidrológico da região. No entanto, mudanças nesses fluxos, especialmente durante as fases do ENSO, alteram a disponibilidade de umidade do solo e, consequentemente, a suscetibilidade ao fogo. Utilizando múltiplos conjuntos de dados (ERA5, GLEAM, GLDAS e CCI SM), o estudo aplica análise de função ortogonal empírica (EOF), análise harmônica, teste de tendência de Mann-Kendall, correlação de Pearson e análise espectral de potência para identificar padrões espaço-temporais dominantes na umidade do solo e nos fluxos de umidade em toda a América do Sul. Os resultados indicam que as fases de El Niño enfraquecem a Zona de Convergência do Atlântico Sul (ZCAS) e reduzem o transporte de umidade da Amazônia, levando a condições mais secas e a um maior risco de incêndios florestais no Cerrado. Em contraste, os eventos de La Niña intensificam a precipitação ao fortalecer os fluxos de umidade amazônicos e atlânticos, mitigando a atividade do fogo. O estudo também avalia o papel das mudanças no uso da terra, do desmatamento e das práticas de manejo do fogo na modificação dos caminhos do fluxo de umidade e na alteração dos regimes naturais de incêndios. Os achados ressaltam a importância da umidade do solo na regulação dos processos hidrológicos e na resiliência dos ecossistemas no Brasil central. À medida que as mudanças climáticas se intensificam, eventos hidrológicos extremos, como secas prolongadas e episódios de precipitação intensa, devem perturbar os balanços de umidade, reforçando a necessidade de monitoramento contínuo e modelagem preditiva. O estudo destaca a necessidade de conservar as florestas amazônicas e implementar práticas sustentáveis de uso da terra para manter os fluxos regionais de umidade e mitigar os riscos de incêndios. Ao aprimorar a compreensão do transporte

de umidade, da variabilidade da umidade do solo e da suscetibilidade ao fogo, esta pesquisa fornece insights valiosos para estratégias de adaptação climática, gestão de recursos hídricos e políticas de prevenção de incêndios no Cerrado.

Palavras-chave: Fluxo de Umidade. Variabilidade da Umidade do Solo. Dinâmica do Fogo. Forçantes Climáticas.

ABSTRACT

SAITO, Youlia Kamei, D.Sc., Universidade Federal de Viçosa, March, 2025. **Spatio-temporal patterns of atmospheric water transport and soil moisture across South America from 1980 to 2020**. Adviser: Flavio Barbosa Justino. Co-adviser: Carlos Diego de Sousa Gurjão.

The Cerrado region of Brazil is a crucial ecological and agricultural zone, significantly influenced by atmospheric moisture fluxes that regulate precipitation, soil moisture, and fire activity. This study analyzes the interactions between soil moisture variability, atmospheric moisture transport, and fire dynamics, considering large-scale climate drivers such as the El Niño-Southern Oscillation (ENSO) and Tropical Atlantic Variability (TAV). Moisture influx from the Atlantic and Pacific Oceans, as well as the Amazon Basin, plays a fundamental role in shaping the region's hydrological balance. However, shifts in these fluxes, particularly during ENSO phases, alter soil moisture availability and, consequently, fire susceptibility. Using multiple datasets (ERA5, GLEAM, GLDAS, and CCI SM), the study applies empirical orthogonal function (EOF) analysis, harmonic analysis, Mann-Kendall trend analysis, Pearson correlation, and power spectrum analysis to identify dominant spatiotemporal patterns in soil moisture and moisture flux across South America. The results indicate that El Niño phases weaken the South Atlantic Convergence Zone (SACZ) and reduce moisture transport from the Amazon, leading to drier conditions and an increased risk of wildfires in the Cerrado. In contrast, La Niña events enhance precipitation by strengthening Amazonian and Atlantic moisture fluxes, mitigating fire activity. The study also assesses the role of land-use changes, deforestation, and fire management practices in modifying moisture flux pathways and altering natural fire regimes. The findings emphasize the importance of soil moisture in regulating hydrological processes and ecosystem resilience in central Brazil. As climate change intensifies, extreme hydrological events such as prolonged droughts and intense precipitation episodes are expected to disrupt moisture balances, reinforcing the need for continuous monitoring and predictive modeling. The study highlights the necessity of conserving Amazonian forests and implementing sustainable land-use practices to maintain regional moisture fluxes and mitigate fire risks. By improving the understanding of moisture transport, soil moisture variability, and fire susceptibility, this research provides valuable insights for climate adaptation strategies, hydrological resource management, and fire prevention policies in the Cerrado.

Keywords: Moisture Flux. Soil Moisture Variability. Fire Dynamics. Climate Drivers.

SUMÁRIO

1 Introdução Geral

A região do Cerrado, no Brasil, frequentemente chamada de “celeiro do país”, é uma zona ecológica e agrícola crítica, com clima e hidrologia profundamente influenciados pelos fluxos atmosféricos de umidade provenientes dos oceanos Atlântico e Pacífico, bem como da Bacia Amazônica. Esses mecanismos de transporte atmosférico são vitais para a regulação da precipitação regional, da dinâmica da umidade do solo e da atividade de incêndios. Uma compreensão aprofundada da complexa interação entre umidade do solo, fluxos atmosféricos de umidade e grandes forçantes climáticos é essencial para prever mudanças ambientais, gerir os recursos hídricos e mitigar os riscos de incêndios florestais nessa região.

A variabilidade dos fluxos de umidade no Cerrado é moldada por processos atmosféricos complexos, incluindo o Sistema de Monção da América do Sul (SMAS), a Zona de Convergência do Atlântico Sul (ZCAS) e grandes oscilações climáticas, como o El Niño–Oscilação Sul (ENOS) e a Variabilidade do Atlântico Tropical (TAV). As flutuações sazonais desses fluxos afetam diretamente a disponibilidade de umidade no solo, o que, por sua vez, influencia a estabilidade dos ecossistemas, a produtividade agrícola e a suscetibilidade a incêndios. Fatores antrópicos, como o desmatamento e a conversão de terras, complicam ainda mais essas relações, ao alterar os caminhos naturais da umidade e os regimes de fogo. A umidade do solo atua como regulador central do balanço hidrológico do Cerrado, controlando o escoamento superficial, a recarga subterrânea e as taxas de evaporação, desempenhando, assim, um papel fundamental nos ciclos de retroalimentação da precipitação em escala local e regional.

Embora estudos anteriores tenham examinado aspectos dessas dinâmicas, ainda falta uma análise abrangente, baseada em múltiplos conjuntos de dados, que integre a umidade do solo, os fluxos atmosféricos de umidade e a dinâmica dos incêndios em toda a América do Sul, a fim de caracterizar plenamente essas interações. Esta tese aborda essa lacuna ao apresentar uma análise integrada dos padrões espaço-temporais do transporte atmosférico de água e da umidade do solo entre 1980 e 2020. A pesquisa está estruturada em torno de dois artigos distintos, mas interconectados.

O primeiro artigo, *“Dinâmica da Umidade do Solo no Brasil: Uma Análise com Múltiplos Conjuntos de Dados de 1990 a 2020”*, concentra-se no papel fundamental da umidade do solo. Ele utiliza diversos conjuntos de dados (ERA5, GLEAM, GLDAS, CCI SM) para identificar a variabilidade sazonal e interanual da umidade do solo, seus padrões dominantes espaciais e temporais, e sua relação com índices climáticos-chave (TAV, ENOS e SMAS). Este artigo estabelece o papel crítico da umidade do solo como variável dinâmica no ciclo hidrológico da América do Sul e sua resposta às forçantes climáticas.

O segundo artigo, *“Respostas dos Fluxos de Umidade da América do Sul aos Oceanos Atlântico e Pacífico e Implicações para a Incidência de Incêndios”*, expande essa base ao investigar como os fluxos de umidade e os forçantes climáticos influenciam a dinâmica dos incêndios no Cerrado. Ele emprega o Modelo de Reciclagem Dinâmica de Duas Camadas (2L-DRM) para quantificar a contribuição de diferentes fontes de umidade para a região-alvo e avalia como fenômenos climáticos como o ENOS e a TAV modulam esses fluxos e sua ligação com a atividade de fogo. Os resultados desse artigo destacam a importância do transporte de umidade proveniente do Atlântico, do Pacífico e da Amazônia para a gestão e a prevenção de incêndios no Cerrado.

Ao integrar os resultados desses dois artigos, esta tese fornece uma compreensão holística das conexões entre transporte de umidade, umidade do solo e incidência de incêndios. A pesquisa oferece percepções essenciais para o desenvolvimento de estratégias de adaptação climática, a implementação de práticas sustentáveis de manejo da terra e a mitigação de riscos de incêndio no Brasil central, com forte ênfase na necessidade de conservar fontes críticas de umidade, como a Bacia Amazônica.

Artigo 1: Soil Moisture Dynamics in Brazil: A Multi-Dataset Analysis from 1990 to 2020

Abstract

Based on ERA5, GLEAM, GLDAS, and CCI SM South America soil moisture variability is investigated. Calculations of harmonic analysis, EOF decomposition, trend evaluation, correlations and spectral analysis, reveal strong regional contrasts in SM patterns driven by major climate systems and modes. Seasonal SM variability is dominated by the migration of the Intertropical Convergence Zone (ITCZ) and the influence of the South Atlantic Convergence Zone (SACZ), especially in the Amazon and central Brazil. EOF results highlight these areas as key centers of variability, reflecting strong coupling between precipitation and SM, with significant implications for agriculture. Trend analysis shows increasing SM in northern regions, while central, northeastern, and southern Brazil exhibit declines, linked to changing rainfall regimes and atmospheric circulation, including the South Atlantic Subtropical High (SASH). In the Northeast, reductions in SM amplify risks related to drought and water scarcity. Power spectral analysis reveals significant periodic components—particularly in GLEAM and GLDAS, associated with ENSO and Tropical Atlantic Variability (TAV), underscoring the role of ocean–atmosphere interactions in SM dynamics.

These findings emphasize the need for multi-source datasets and robust analyses to understand and anticipate SM changes critical to agriculture, water resources, and climate resilience in South America.

Keywords: Soil moisture dynamics, Climate variability, Extreme events, Climate Change

1 Introduction

Soil moisture (SM) changes in South America have profound implications for the continental socio-economic and environmental well-being. Agriculture, which constitutes a significant portion of the economy, relies heavily on adequate soil moisture for optimal crop growth and yield (Gouveia et al., 2023; Da Silva e Souza et al., 2020). Moreover, Brazil's diverse ecosystems, from the Amazon rainforest to the

Cerrado and Caatinga biomes, depend on suitable SM levels to maintain biodiversity and ecosystem services. Variations in soil moisture also impact water availability for human consumption, industrial activities, and energy generation, due to large hydropower dependence of the country. Understanding soil moisture changes is, therefore, crucial for mitigating the impacts of climate change, such as those related to droughts and floods, which have become more frequent and severe in many parts of South America (Gouveia et al., 2023, Ávila et al., 2020). Understanding soil moisture dynamics is crucial for decision-makers to effectively manage agriculture, water resources, conservation efforts, and climate adaptation strategies.

Ecological processes crucial for life on Earth are tightly dependent on SM amount. The SM importance lies in multifaceted impacts on agriculture, water resources, biodiversity, and climate regulation (O'Donnell and Manier, 2022). Soil moisture directly influences crop growth, nutrient availability, and water uptake by plants (Rasheed et al., 2022). Adequate soil moisture levels are necessary for germination, root development, and overall plant health. Conversely, excessive moisture can lead to water logging and root rot, affecting the crop yields (Walne and Reddy, 2021).

Furthermore, SM regulates the hydrological cycle by modifying infiltration rates, groundwater recharge and surface runoff, thereby influencing water availability for human consumption and ecosystem services (Guo et al., 2023). Changes in soil moisture can alter vegetation patterns, affect species distribution, and exacerbate habitat loss, ultimately impacting ecosystem stability and services (Lóczy, 2023).

Several factors influence soil moisture dynamics. This includes precipitation, temperature, soil texture, vegetation cover, topography, and human activities (Rasheed et al., 2022; Guo et al., 2023). Precipitation is generally the primary driver of soil moisture variability, directly affecting infiltration rates and soil water content (Guo et al., 2006). Temperature influences evaporation and transpiration rates, which induces change in the balance between water inputs and outputs in the soil system (Zhang et al., 2020). Soil texture, characterized by the proportion of sand, silt, and clay, determines water retention capacity and drainage properties (Upadhyay and Raghubanshi, 2020). On the other hand, vegetation cover affects interception,

evapotranspiration, and litter decomposition rates, thereby, modulating soil moisture levels (Yang et al., 2018).

South America's climate is influenced by a variety of dynamic systems that shape regional precipitation and soil moisture trends. The South Atlantic Convergence Zone (SACZ) significantly increases rainfall in the south and southeast during DJF and MAM, while the Intertropical Convergence Zone (ITCZ) enhances precipitation in northern regions. Conversely, the continental expansion of the South Atlantic Subtropical High (SASH) often induces drought conditions in Brazil, particularly during JJA and SON. Cold fronts bring rain to southern Brazil in MAM and JJA, while Upper Tropospheric Cyclonic Vortices (UTCVs) increase precipitation in Northeast Brazil. The Moisture Convergence Zone fosters rising soil moisture and precipitation in central areas, especially in DJF and MAM. Additionally, Easterly Waves contribute to rainfall in Northeast Brazil during MJJ and JJA, and both the Continental and Atlantic Equatorial Masses influence precipitation patterns, with the Atlantic equatorial air mass enhancing moisture in northern and northeastern regions, particularly during DJF and MAM.

In tropical South America, seasonal rainfall and soil moisture patterns are governed by a suite of dynamic climate systems—chiefly the South Atlantic Convergence Zone (SACZ), the Intertropical Convergence Zone (ITCZ), and the semi-permanent South Atlantic Subtropical High (SASH)—which collectively orchestrate distinct wet and dry seasons across Brazil (Silva et al., 2021; Chug et al., 2022). For example, the high rainfall variability in Northeast Brazil arises from the combined influence of equatorial Atlantic moisture convergence (associated with the seasonal migration of the ITCZ), periodic easterly wave disturbances, and upper-tropospheric cyclonic vortices (UTCVs), along with the shifting position of the SACZ; together, these mechanisms modulate regional precipitation patterns and consequent soil moisture dynamics (Bernardino et al., 2017; Silva et al., 2021).

The relationship between soil moisture and precipitation is complex and dynamic, involving feedback mechanisms that vary across different spatial and temporal scales (Sehler et al., 2019). Precipitation directly replenishes SM through infiltration and percolation processes, increasing water availability for plants and other organisms. In contrast, SM influences precipitation patterns by affecting atmospheric

moisture content, surface albedo, and convective processes (Jiang et al., 2022; Arsego et al., 2023). Climate variability and change are also altering precipitation patterns, temperature regimes, and extreme weather events, thus, influencing soil moisture dynamics and environmental processes (Skendzic et al., 2021). According to Qin et al. (2023), changes in soil moisture will deteriorate the global water cycle and enhance the variability of extreme meteorological disasters, affecting agricultural productivity, water and food security, and ecosystem integrity (Furtak and Wolińska, 2023). Changes in soil moisture can amplify feedback loops, further increasing climate change impacts and posing challenges for adaptation and mitigation strategies (Thompson et al., 2022; Jiang et al., 2023). Indeed, Jucá et al. (2002) demonstrated that overall soil moisture in Brazil has declined by 0.5\% yr^{-1} (p\textless0.01) at the country level from 2009 to 2015. At the biome level, Caatinga has been most affected with SM reduction (−4.4\% yr^{-1}), whereas the Atlantic Forest and Cerrado biomes delivered no significant trends.

To analyze soil moisture dynamics across South America, this study applies four datasets (ERA5, GLEAM, GLDAS, CCI SM) from January 1990 to December 2020. The present study contributes to previous evaluation by (1) Spennemann et al. (2015), which assesses the reliability of the GLDAS system with four land surface models, (2) Solander et al. (2020) that investigated the pantropical response of soil moisture to El Niño, (3) analyses by Jucá et al. (2022) that estimates soil moisture at different depths in the Northeast Brazil, and among many others, Collini et al. (2008) which discusses the feedbacks between soil moisture and precipitation during the early stages of the South American monsoon. Herein, it is investigated the SM seasonal and interannual variability, the dominant spatial and temporal patterns, and its relationship with key climate indices such as the Tropical Atlantic Variability (TAV), the El Niño-Southern Oscillation (ENSO), and the South America Monsoon (SAM). These analyses are conducted by employing cross-correlations, harmonic analysis, empirical orthogonal function (EOF), Mann-Kendall evaluation, and power spectrum analysis.

2 Material and Methods

2.1 Soil Moisture and Precipitation Data

Monthly data between January 1990 to December 2020 based on distinct platforms are used to investigate soil moisture dynamics, and ERA5 is chosen for characterizing the link between precipitation and SM. The SM datasets include GLEAM (Global Land Evaporation Amsterdam Model), GLDAS (Global Land Data Assimilation System), and CCI SM (Climate Change Initiative Soil Moisture) and ERA5 for soil moisture. The main characteristics of the precipitation and soil moisture datasets are summarized in Table 1.

ECMWF reanalysis v5 (ERA5)

ERA5 is the fifth-generation atmospheric reanalysis dataset produced by the European Centre for Medium-Range Weather Forecasts (Hersbach et al., 2020, ECMWF). It assimilates a wide range of observations from satellites, ground-based stations, and other sources into a global atmospheric model to produce consistent estimates of various meteorological parameters, including soil moisture and precipitation. The spatial resolution is approximately 0.25 degrees globally and the data are provided hourly and monthly. The data are sourced from the ECMWF (https://cds.climate.copernicus.eu/). The soil moisture values are based on the top 7 centimeters of soil, as simulated by the Hydrology Tiled ECMWF Scheme for Surface Exchanges over Land (HTESSEL) model. This model uses various soil texture classes with unique properties, such as infiltration capacity and wilting point. To ensure accuracy, calculations exclude regions with permanent ice cover (like Antarctica and most of Greenland) or no vegetation.

GLDAS - Land Data Assimilation System (LDAS NASA)

GLDAS is a land surface modeling and data assimilation system that combines satellite and ground-based observations with land surface models to estimate various land surface variables, including soil moisture. It assimilates observational data from

multiple satellite missions and ground stations to produce gridded datasets. A remarkable implementation of GLDAS is the use of soil texture classification schemes that specify soil parameters based on texture classes, while others derive soil hydrologic and thermal properties from sand, clay, and silt fractions. The GLDAS provides global coverage at a spatial resolution of approximately 0.25 degrees. The data are sourced from the Land Data Assimilation System (LDAS NASA) (https://ldas.gsfc.nasa.gov/gldas/gldas-get-data). This study uses two versions of the GLDAS: from 1990-2000 the version 2 and therefrom the version 2.1. For additional detail the reader is invited to visit https://disc.gsfc.nasa.gov/datasets/GLDAS_NOAH025_3H_V2.1/summary.
According to Spennemann et al. (2015), the use of the global meteorological forcing dataset from Princeton University in GLDAS-v2, and the Noah LSM that includes land surface parameters based on the Moderate Resolution Imaging Spectroradiometer (MODIS) and the Advanced Very High Resolution Radiometer (AVHRR) instead of using only the AVHRR, as in GLDAS-1 and GLDAS-2 (v1), result in a better representation of soil conditions in GLDAS-v2.

GLEAM - Global Land Evaporation Amsterdam Model

GLEAM is a satellite-based dataset that estimates land surface evaporation and its components, including soil moisture. It integrates satellite observations of meteorological variables, such as temperature, radiation, and vegetation indices, into a water balance model to estimate soil moisture dynamics (Martens et al., 2017). GLEAM provides global coverage at a spatial resolution of 0.25 degrees.The data are sourced from the GLEAM (https://www.gleam.eu/). GLEAM utilizes satellite-derived soil moisture data from active C- and L-band microwave sensors (European Space Agency Climate Change Initiative, ESA CCI), along with vegetation optical depth, snow-water equivalent, reanalysis air temperature and radiation, and a multi-source precipitation product. According to Martens et al. (2017), GLEAM's soil moisture correlations with in situ surface soil moisture measurements average around 0.64, while its evaporation fluxes show correlations with eddy-covariance data ranging from 0.78 to 0.81, depending on location. This demonstrates GLEAM's capability in

accurately representing terrestrial fluxes across diverse ecosystems, as evidenced by Lu et al. (2021).

CCI SM - Climate Change Initiative

This dataset is derived from satellite observations. The ESA-CCI Soil Moisture dataset combines passive and active microwave measurements from various satellite missions, such as ESA's Soil Moisture and Ocean Salinity (SMOS), and NASA's Soil Moisture Active Passive (SMAP). These satellites measure microwave emissions from the Earth's surface, which can be related to soil moisture content. The dataset provides global coverage at a spatial resolution of approximately 0.25 degrees (~25 km). The data are sourced from the European Space Agency (https://climate.esa.int/en/projects/soil-moisture/).

It should be mentioned the lack of data across western Amazon which can be attributed to uncertainties due to the dense vegetation cover of the Amazon. This interferes with the accuracy of soil moisture data obtained by the satellite, making data interpretation more difficult or requiring specific processing methods.

Table 1. Summary of selected gridded monthly precipitation and soil moisture datasets.

Abbreviation	Dataset	Spatial Resolution	Sources
ERA5	ERA5 monthly averaged data on single levels from 1940 to present	0.25°	https://cds.climate.copernicus.eu/cdsapp#!/dataset/reanalysis-era5-single-levels-monthly-means?tab=overview
GLEAM	GLEAM v3.8a	0.25°	https://www.gleam.eu/
GLDAS	GLDAS_NOAH025_M 2.0 GLDAS_NOAH025_M 2.1	0.25°	https://disc.gsfc.nasa.gov/datasets?keywords=GLDAS
CCI SM	SA CCI SM v08.1	0.25°	https://climate.esa.int/en/projects/soil-moisture/

2.2 Methods

Statistical methods are carried out to characterize the spatio-temporal features of soil moisture, and its potential link with precipitation. Harmonic analysis decomposes the time series into a series of sine waves, allowing us to pinpoint key characteristics in space and time. It extracts the amplitude, indicating the intensity of seasonal swings, the variance, showcasing the data's variability, and the phase, marking the timing of seasonal peaks. By using the least squares fitting method, it isolates the most prominent harmonic components, providing a clearer understanding of the underlying seasonal shifts. Harmonic analysis is a valuable tool for characterizing climate regimes and transition zones. The first-order harmonics of meteorological parameters reveal dominant patterns, while higher-order harmonics capture short-term fluctuations. The phase angle indicates the timing of maximum or minimum values for a given harmonic. By decomposing meteorological data into its harmonic components, we can identify dominant climate features in both space and time.

EOF analysis, on the other hand, is a powerful method for uncovering dominant patterns within large datasets (Yue et al., 2020). By decomposing spatiotemporal data into orthogonal basis functions, this method isolates key patterns and their associated temporal variations (Wang et al., 2017). The process involves: (1) Normalization: to standard data to have zero mean and unit variance; Covariance Matrix: to calculate the covariance matrix of the normalized data; (2) Eigenvalue Decomposition: to determine the eigenvalues and eigenvectors of the covariance matrix; (3) EOF Modes and Principal Components identify the spatial patterns (EOF modes) represented by the eigenvectors and the temporal variability (principal components). We applied EOF analysis to the anomaly fields for annual, summer, and winter periods. In order to compute trends, the Mann-Kendall analysis is used. The results of the first component (PC1) obtained in the EOF analysis is subjected to the Mann-Kendall test in order to find trends. This test is widely used to detect monotonic trends in hydrometeorological data, such as precipitation and soil moisture (Santos et al., 2020; Lornezhad et al., 2023; Mohseni et al., 2023). The nonparametric assumption is robust against outliers and does not require assumptions about data distribution, making it suitable for trend analysis in environmental datasets (Zeng et al., 2019).

The Mann-Kendall test determines if a trend exists within a time series. It involves: (1) Data Ranking: to assign ranks to data points based on their temporal order. (2) Statistic Calculation: to calculate the S statistic, which measures the number of positive differences minus the number of negative differences. (3) Significance Assessment: to evaluate the significance of the trend using the standard normal variable, derived from the S statistic. This test provides valuable insights into the direction and strength of changes over time.

The Pearson correlation coefficient is a statistical measure that evaluates the strength and direction of the linear relationship between two variables. In this study, we apply Pearson correlation analysis to understand the relationship between soil moisture and precipitation data under different lead/lags occurrences. This methodology provides insights into how climatic variability influences hydrological variables, across different temporal and spatial scales. The Pearson correlation coefficient (r) is computed for pairs of variables at each grid point across the study region. The coefficient is given by:

$$r = \frac{\sum_{i=1}^{n}(X_i - \bar{X})(Y_i - \bar{Y})}{\sqrt{\sum_{i=1}^{n}(X_i - \bar{X})^2 \sum_{i=1}^{n}(Y_i - \bar{Y})^2}} \quad (1)$$

where X and Y are the variables (e.g., soil moisture and climate index values), and $\bar{X}$ and $\bar{Y}$ are their respective means (Xu and Deng, 2018).

Power spectrum analysis is used to examine the frequency characteristics of soil moisture variability. This method helps identify dominant periodicities and the distribution of variance across different frequency bands, providing insights into the temporal dynamics of soil moisture as influenced by climate variability and other factors. The spectrum analyses are applied on 1st and 2nd principal components delivered by the EOFs technique.

Power Spectrum Calculation is based on the Fourier Transform to convert the time series data from the time domain to the frequency domain. The Discrete Fourier Transform (DFT) is used for this purpose, given by:

$$X(f) = \sum_{t=0}^{N-1} x(t) e^{-i2\pi ft/N} \quad (2)$$

where x(t) is the 1st and 2nd PC soil moisture time series, N is the number of observations, and f is the frequency. The power spectrum P (f) is calculated as the squared magnitude of the Fourier coefficients:

$$P(f) = |X(f)|^2 \quad (3)$$

This provides the distribution of power (variance) across different frequency components. To obtain a smoothed representation of the power spectrum, spectral density estimation techniques such as the Welch method are used. This involves dividing the time series into overlapping segments, computing the periodogram for each segment, and averaging the results. The power spectrum is normalized by the total variance of the time series to facilitate comparison across different datasets and regions. Statistical significance of the spectral peaks is assessed using the red noise spectrum as a background spectrum. Peaks that rise above the red noise spectrum are considered significant.

Climate Index

Further research is essential to understand the impact of oceanic variability on surface climate and in particular to SM. Patterns associated with the South America Monsoon (SAM), the Tropical Atlantic Variability (TAV), the El Niño-Southern Oscillation (ENSO) can significantly modify the SM spatial pattern and magnitude. These oceanic phenomena induce anomalies in precipitation and temperature leading to changes in environmental conditions far from their origins (Justino et al., 2022).

South American Monsoon (SAM)

The SAM is a key climatic feature influencing the distribution of rainfall in Brazil, especially during the summer months (Nielsen et al., 2016, Gurjão et al., 2023). The SAM is characterized by a seasonal reversal in wind patterns and a significant increase in precipitation (Santos et al., 2014). This system primarily affects the Central-West, Southeast, and parts of the Northeast regions of Brazil. During the wet season, SAM leads to a substantial increase and subsequently in precipitation and soil moisture in these areas (Carvalho and Jones, 2016). Conversely, during the dry season (winter), precipitation decreases, resulting in lower soil moisture levels (Carvalho and Jones, 2016).

El Niño-Southern Oscillation (ENSO)

The ENSO phenomenon includes two main phases: El Niño and La Niña, along with a neutral phase. In Brazil, El Niño typically leads to reduced rainfall in the North and Northeast regions, causing drought conditions and lower soil moisture (Costa et al., 2020; Kay et al., 2022). In the South, El Niño can lead to increased rainfall, thus enhancing soil moisture (de Souza et al., 2021). Conversely, during La Niña events, the equatorial Pacific Ocean waters are cooler than average, increasing rainfall in the North and Northeast of Brazil, leading to higher soil moisture levels (Rodrigues and McPhaden, 2014). In the South, La Niña can cause reduced rainfall and lower soil moisture.

Tropical Atlantic Variability (TAV)

The TAV refers to the variations in sea surface temperatures (SST) in the tropical Atlantic, which influence climatic patterns in Brazil. The negative SST anomalies in the northern tropical Atlantic are associated with increased convective activity in the North and Northeast of Brazil, resulting in higher precipitation and increased soil moisture in these regions. Utida et al., (2019) indicate that regional precipitation along South America's coast was not solely influenced by the north-south movement of the Intertropical Convergence Zone (ITCZ), in response to Northern Hemisphere climate changes. The contraction and expansion of the tropical rainbelt, driven by variations in sea surface temperature and southeast trade winds within the tropical South Atlantic basin, also played a significant role. The positive SST anomalies in the southern tropical Atlantic therefore enhance moisture convergence and increase rainfall in the Southeast and South of Brazil, leading to higher soil moisture levels in these areas (Bernardino et al., 2017).

These climatic systems do not operate in isolation, and their interactions can produce all sorts of precipitation and soil moisture patterns. For example, the interaction between ENSO and TAV can significantly modify expected climatic impacts in certain regions, such as northeastern Brazil and parts of the Amazon (Kayano et al., 2011). Additionally, other systems such as the South Atlantic Convergence Zone (SACZ) and cold fronts also play important roles in modulating precipitation and soil moisture in Brazil (Bernardino et al., 2017), in association with those oceanic modes of climate variability.

The impact of the South America Monsoon (SAM), ENSO and TAV on soil moisture is analysed through the technique of maximum lag correlation based on autoregressive vectors, which consists of providing the maximum correlation coefficients between the soil moisture patterns and the climate indices, and the corresponding time lag (Song et al., 2019). The lag correlation coefficient between the two series X(n) and Y(n) is defined by equation 7 (Eq. 7), where τ is the time lag, $\bar{x}$ and σ_x are the mean and standard deviation of series x, and $\bar{y}$ and σ_y are the mean and standard deviation of series y, respectively.

$$Lag_{Corr}(\tau) = \frac{1}{n-\tau} \cdot \sum_{k=1}^{n-\tau} \left\{ \left[\frac{x(k)-\bar{x}}{\sigma_x} \right] \cdot \left[\frac{y(k+\tau)-\bar{y}}{\sigma_y} \right] \right\} \quad (4)$$

3 Results

3.1 Seasonality

Figure 1 shows the first harmonic amplitude, phase and variance delivered by the four datasets. Analysis of the amplitudes shows the strength of the SM seasonal cycle. In the North and Central parts of Brazil, a strip of higher amplitudes are noticed across these regions, indicating strong seasonal changes in soil moisture. This is noticed in particular for ERA5 and CCI SM (Fig. 1a,b). Across the northern part SM is significantly influenced by the ITCZ, which changes seasonally and brings substantial rainfall during its passage. In the Amazon CCI SM, as previously mentioned, experiences a lack of data due to the dense vegetation which hampers a proper application of the algorithm (Fig. 1b). However, it is evident that the western parts of the Amazon basin soil moisture is barely affected by seasonality. Strictly speaking, the Amazon basin displays notable spatial variability in soil moisture amplitude across both west-east and north-south axes. This variability is driven by several key factors. First, the South Atlantic Convergence Zone (SACZ) plays a significant role, particularly in the southern and southeastern regions, where it brings heavy rainfall and leads to elevated soil moisture levels (Chug et al., 2022). Second, the Intertropical Convergence Zone (ITCZ) influences the northern Amazon, with its seasonal north-south shifts contributing to soil moisture variability along this axis (Marengo et al., 2009, 2015).

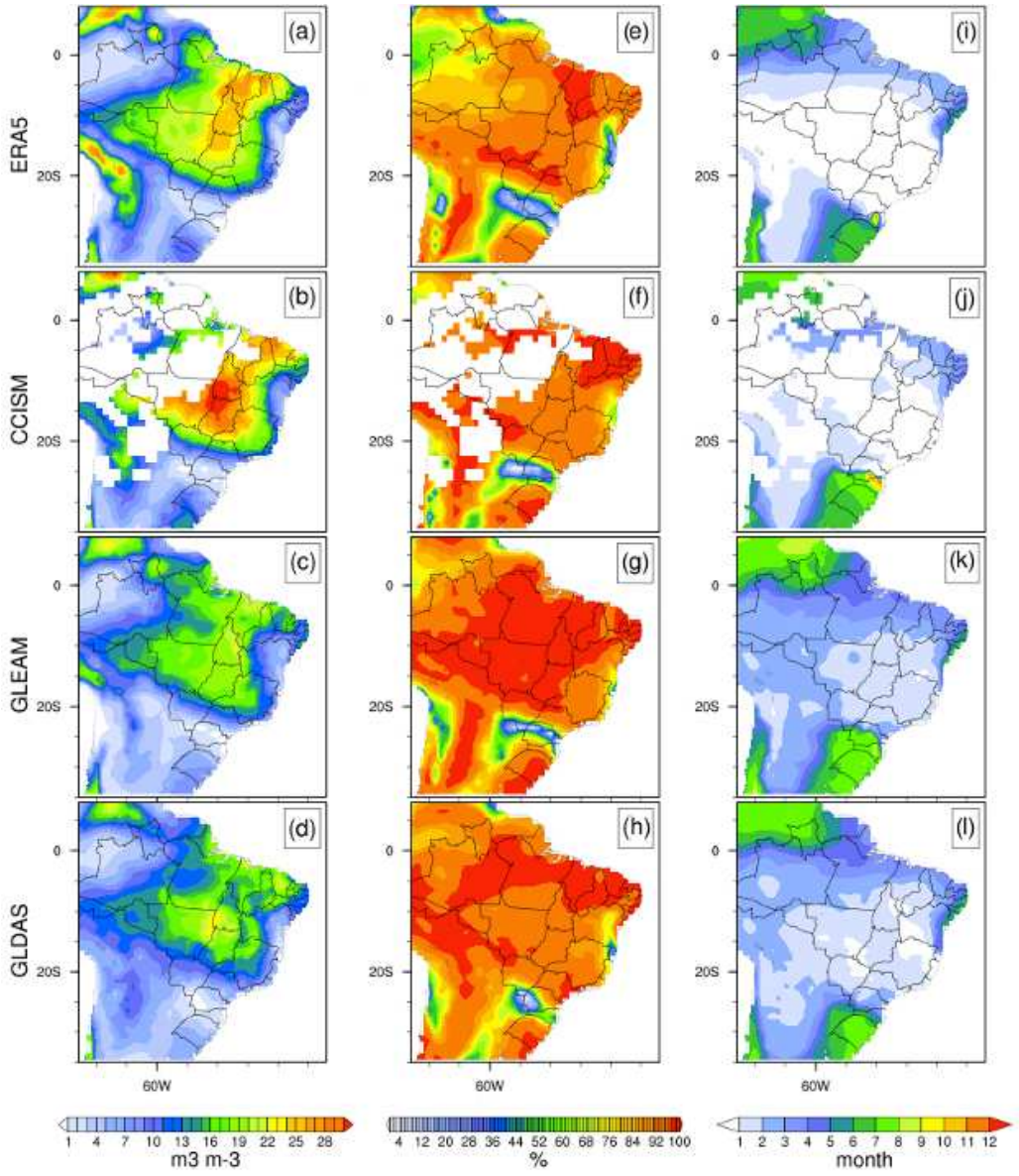

Figure 1: Harmonic analysis of soil moisture data from ERA5, CCI, GLEAM and GLDAS. a, b, c, d are amplitudes of the first harmonic; e, f, g, h are variance; and, i, j, k, l are phases, respectively.

The northeastern coast of Brazil (NEB), similarly, is characterized by lower amplitude values, demonstrating smaller seasonal changes in SM compared to other regions. During the rainy season, several disturbances including easterly waves, Upper Tropospheric Cyclonic Vortexes (UTCV) and the South Atlantic Convergence Zone (SACZ) induce rainfall patterns in the NEB. The Atlantic Forest, furthermore, a permanent source of moisture, which combined with maritime air advected by the sea breeze, contributes to a consistent local precipitation regime along the Brazilian coast.

However, the central part of Brazil experiences a more pronounced seasonal cycle due to the influence of the South America Monsoon (SAM) and other atmospheric systems embedded within it. Additionally, the region's diverse topography and vegetation further contribute to these variations, as areas with differing elevations and vegetation types affect water retention. Wind patterns and atmospheric circulation, especially trade winds, interact with local topography to create precipitation gradients (Santos et al., 2014) further shaping the spatial distribution of soil moisture throughout the basin.

Among the amplitudes delivered by the datasets, it is noticed that with respect to GLEAM and GLDAS (Fig. 1c,d), CCI and ERA5 (Fig. 1a,b) show higher amplitudes in the north and central region of Brazil, especially in the Amazon and the Cerrado regions. The CCI SM presents amplitude patterns similar to ERA5, but with higher values in some areas of central Brazil, indicating a greater sensitivity to temporal changes of precipitation events. The GLEAM shows a more homogeneous distribution of amplitudes, with strong seasonal variations across eastern Amazon, Cerrado and western NEB. The GLEAM methodology, which focuses on modeling evapotranspiration based on observations, can be the cause of these differences. Evaporation/transpiration is highly dependent on surface temperatures which across central Brazil do not substantially change their spatial distribution. GLDAS (Fig. 1d) presents similar results to GLEAM, but with more defined areas of higher amplitude. Integrating different models into GLDAS can result in a more balanced but less extreme representation of amplitudes (Spennemann et al., 2015).

Amplitude analyses, as discussed above, should be linked to the variance explained by the 1st harmonic (Figs. 1e-h). It is very clear that across most parts of Brazil the SM is dictated by the seasonal cycle, with variance higher than 80%. However, larger variance is delivered by the GLEAM. It may be argued that ERA5, CCI and GLDAS respond to higher frequency inputs due to the assimilation scheme which captures lower order harmonics. A fact that can be absent in GLEAM that is more strongly affected by seasonality. Two areas also stand out showing SM relation to short-term precipitation events, the southern Brazil and southeastern NEB, where the variance is below 35%. Recurrent frontal systems and meso-scale convective clusters move onto these regions producing rainfall throughout the year, weakening the seasonal relevance. The phase maps (Figs. 1i–l) reveal the timing of peak soil

moisture. In Northern Brazil, peak soil moisture occurs in April and May, coinciding with the northward migration of the ITCZ. Along the NEB's coastal region, peak soil moisture is observed during the winter. Similar patterns are evident in the extreme south and north of Brazil (greenish regions).

Comparing the phase maps, ERA5 (Fig. 1i) and CCI (Fig. 1j) exhibit similar patterns. GLEAM and GLDAS (Fig. 1k,l) indicate peak soil moisture in central Brazil between February and March, while ERA5 and CCI show peaks in January. These discrepancies may be attributed to differences in the precipitation input among the models, and in particular the South America Monsoon rainfall. Additionally, the ability of these SM models to accurately simulate soil evaporation and water retention plays a crucial role in the SM accumulation amount.

3.2 EOF Dominant Pattern

The EOF maps for precipitation and soil moisture reveal the dominant patterns of variability across months, separately analyzed for the summer (DJFM) and winter (JJAS) seasons (Fig. \ref{fig2}). These spatial patterns highlight regions where interannual variability is most pronounced, potentially linked to key climate systems influencing Brazil. When considered seasonally, the variance explained by the first principal component increases (annual = 14.1\%, summer = 22.2\%, winter = 20.6\%), reflecting the strong seasonal control on both precipitation and soil moisture.

On the annual scale, the leading precipitation pattern exhibits a dipole-like structure between northern South America and central Brazil. This configuration suggests the influence of the Intertropical Convergence Zone (ITCZ), along with teleconnections involving ENSO, the Atlantic Multidecadal Oscillation (AMO) the Pacific Decadal Oscillation (PDO), and the Atlantic subtropical high, which becomes more prominent during winter (Fig. 2a,c) (Grimm and Saboia, 2015).

During summer (DJFM), the South American Monsoon (SAM) system drives enhanced precipitation over central Brazil, while suppressing rainfall over the equatorial belt and the Amazon Basin (Fig. 2b). In contrast, the winter (JJAS) pattern features a precipitation core centered between 20°S and 30°S, in opposite phase to equatorial precipitation anomalies (Fig. 2c). This signal is associated with the intensified and

westward-expanded Atlantic subtropical high, which often leads to atmospheric blocking conditions. These blocks inhibit rainfall across central Brazil but can favor stationary frontal systems in the subtropical regions, enhancing precipitation in those areas.

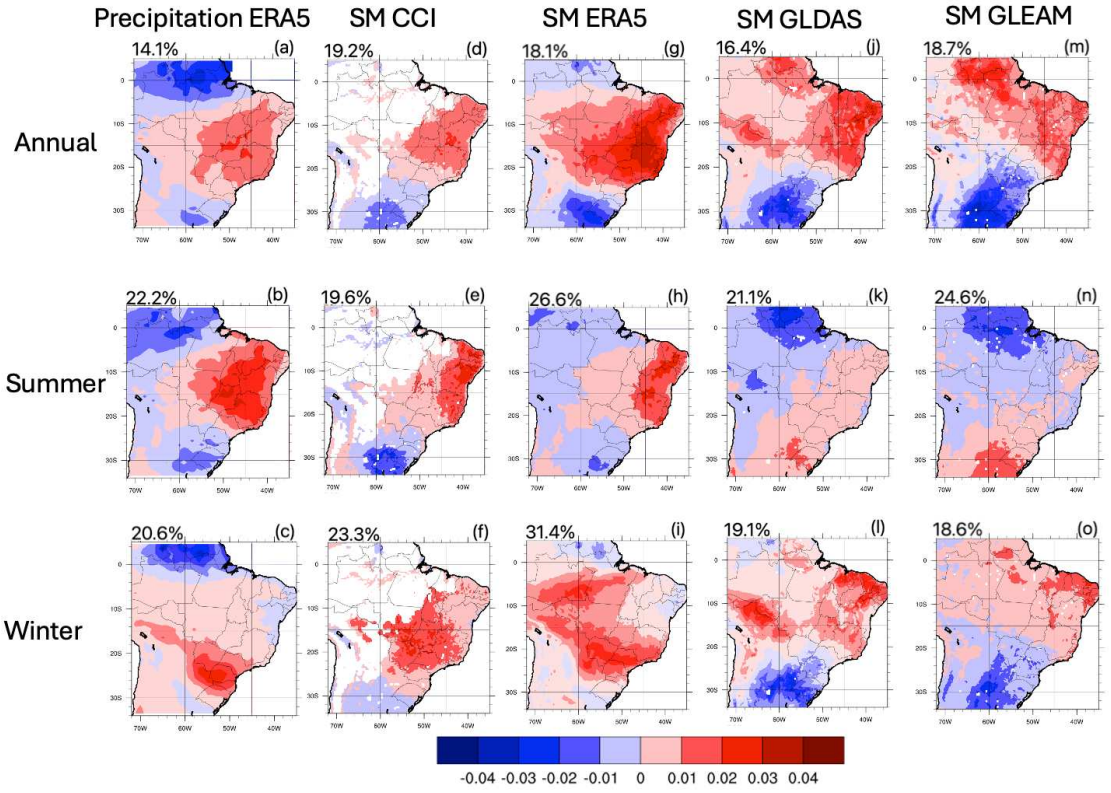

Figure 2: First EOF for Precipitation (ERA5) and Soil Moisture (CCI, ERA5, GLDAS, GLEAM) for Annual, Summer, and Winter Seasons over South America

Interestingly, all datasets show a reasonable agreement along the eastern coast of South America, suggesting more reliable SM estimates in this region. This may be attributed to higher observational coverage; for instance, CCI SM exhibits a valid observation fraction between 0.6 and 0.8 in this area (Dorigo et al., 2015). Despite these improvements, Fang et al. (2016) highlighted that satellite-based SM estimates still show lower correlations than those obtained from in situ observations and land surface model simulations integrating observed precipitation. A key limitation lies in the mismatch between the depth of in situ sensors and the effective depth sensed by satellite products, complicating direct comparisons. Seasonal analyses of SM show that during summer (DJFM), a dominant pattern emerges along the eastern coast of South America, especially in the CCI and ERA5 datasets.

In contrast, GLDAS and GLEAM show weaker signals in this region and instead highlight negative anomalies in the equatorial Northern Hemisphere (Fig. 2, middle panels). Precipitation patterns during this season are characterized by strong variability over central Brazil, driven by the South Atlantic Convergence Zone (SACZ) and the South American Monsoon (SAM). Over the NEB, precipitation—and consequently SM—is influenced by the ITCZ and possibly by easterly wave disturbances, all of which modulate SM variability. In winter (JJAS), the leading SM pattern extends over much of central South America, including the western Amazon (Fig. 2, bottom panels). GLEAM and GLDAS reveal enhanced meridional gradients between subtropical and tropical regions, a feature less evident in CCI and ERA5. Variability in southern Brazil, Argentina, and Uruguay is largely driven by frontal systems that increase precipitation and, consequently, SM.

Overall, SM patterns appear to be shaped predominantly by large-scale, seasonally varying atmospheric systems. The following section explores the temporal evolution of precipitation and SM through seasonal trend analyses to assess the extent to which each dataset captures long-term changes. By analyzing the annual SM distribution (Fig. 2b,c,d,e), it is clear that the tropics and the subtropics are characterized by an out$-$of$-$phase behavior, in which the magnitude is dependent on the dataset. Indeed, GLDAS and GLEAM exhibit an homogeneous region in the NEB and northern equatorial South America, larger than that predicted to occur by the ERA5 and CCI (Fig. 2, top panels). This is interesting because despite a good representation of precipitation by ERA5 related to the ITCZ, the SM does not respond similarly, insofar as the spatial distribution is concerned. This is also observed based on the CCI SM.

It should be mentioned that the match among all datasets along the SA east coast may indicate that across this region SM is well reproduced, in particular because, according to Dorigo et al., (2015), the fraction of days with valid observations of CCI SM is between 0.6 and 0.8. Despite these improvements, Fang et al., (2016) demonstrated for several networks that correlations still lower than that obtained for in-situ data and Land Surface Models simulations, integrating observed precipitation. It is worth noting that in many situations that depth of in situ sensors is different from the typical depth represented by the band satellite product, which hampers a proper comparison.

Analyses for summer and winter SM show that in the former, there exists a dominant pattern along the east coast in particular for CCI and ERA5, which is much weaker in GLDAS and GLEAM, that are characterized by negative regions in the equatorial domain of the Northern Hemisphere (Fig. 2, middle panels). Respective precipitation shows, as expected, strong variability in central Brazil, linked to the SACZ and SAM. On the other hand, the variability across the NEB is influenced by the ITCZ and may also reflect easterly waves. All these phenomena indirectly affect the SM temporal characteristics.

In winter, the dominant pattern covers most of central South America (Fig. \ref{fig2} bottom panels), including western Amazon. The GLEAM and GLDAS datasets do show enhanced meridional seesaw gradients between the subtropics and the tropics, which is not delivered by CCI and ERA5. The variability in southern Brazil, Argentina and Uruguay is related to the presence of frontal systems that induce precipitation and subsequently increase the SM amount. It has to be mentioned that in general, the SM is dominated by large$-$scale features related to seasonal atmospheric systems. The next section deals in detail with trimestral trends of precipitation and SM, in order to verify changing in time characteristics that may be delivered by those distinct datasets.

3.3 Trends of Precipitation and Soil Moisture

Precipitation trend maps based on ERA5 (Fig. 3) reveal upward trends across the northern and western Amazon regions but decreasing trends are overall evident in large parts of South America. From SON to FMA significant negative trends are highlighted primarily over the centra-east South America, a highly populated region with substantial agricultural productivity. Situation is more critical from JJA, the dry season in central Brazil, where downwards SM trends are generalized.

Turning to the soil moisture (SM) maps, the ERA5 data reveals significant trends related to the analyzed trimesters (Figs. 3, lower panels). Notably, the eastern regions of Brazil from JFM to JJA (Figs. 3a-f, lower panels) have experienced a reduction in SM, which does not fully align with the precipitation trends (Figs. 3, upper panels). This contrasts with the strong correlation observed for positive trends between precipitation and SM, particularly in northern South America and the western Amazon. From MAM to ASO, a notable decline in SM is observed, closely following precipitation trends. The

most affected region is the western Amazon (0-10°S, 70°W-55°W). Additionally, as the dry season progresses in southern Brazil, more pronounced negative SM trends are evident (Figs. 3j-l, lower panels).

Analyzing the other SM dataset reveals that GLEAM data (Fig. 4, top panels) exhibits a spatial distribution of both increasing and decreasing trends, characterized by predominantly non-significant values across South America. Notably, significant downward trends are observed in the eastern part of the continent around 20°S. Overall, the main pattern presented by GLEAM differs markedly from that of ERA5. These discrepancies likely stem from the differing methodologies: GLEAM relies on satellite data for precipitation, radiation, and vegetation, combined with soil characteristics, to model soil moisture at a 0.25° spatial resolution. In contrast, ERA5 integrates model simulations with a broad range of satellite and in-situ observations through data assimilation, enhancing the accuracy and reliability of its soil moisture estimates. Thus, the distinct input data and methodologies are key factors contributing to these differences.

Turning to the SM.CCI dataset (Fig. 4, middle panels), it is evident that much of western South America lacks consistent trends, largely due to data unavailability, as discussed previously. This gap stems from the absence of satellite observations in the early stages, resulting in incomplete time series. Additionally, passive microwave observations are impacted by factors such as heavy rainfall and dense vegetation, which can interfere with soil moisture retrievals and reduce data reliability in certain regions and seasons. Despite these limitations, the CCI aligns well with ERA5, overall and across small areas exhibiting upward soil moisture trends in the northeastern region and the 20°-30°S latitudinal belt. The GLDAS consistently shows widespread trends of decreasing soil moisture during all trimesters analyzed, with the exception of DJF and JFM (Fig. 4d,e bottom panels). This SM dataset assimilates various observations, such as precipitation, temperature, and radiation, to drive land surface models (LSMs). Main differences with ERA5 and CCI are noticed insofar as the magnitude of trends are concerned. Large discrepancies are also found across the western South, whereas the GLDAS delivers positive trends , conditions that have been delivered by the other SM datasets.

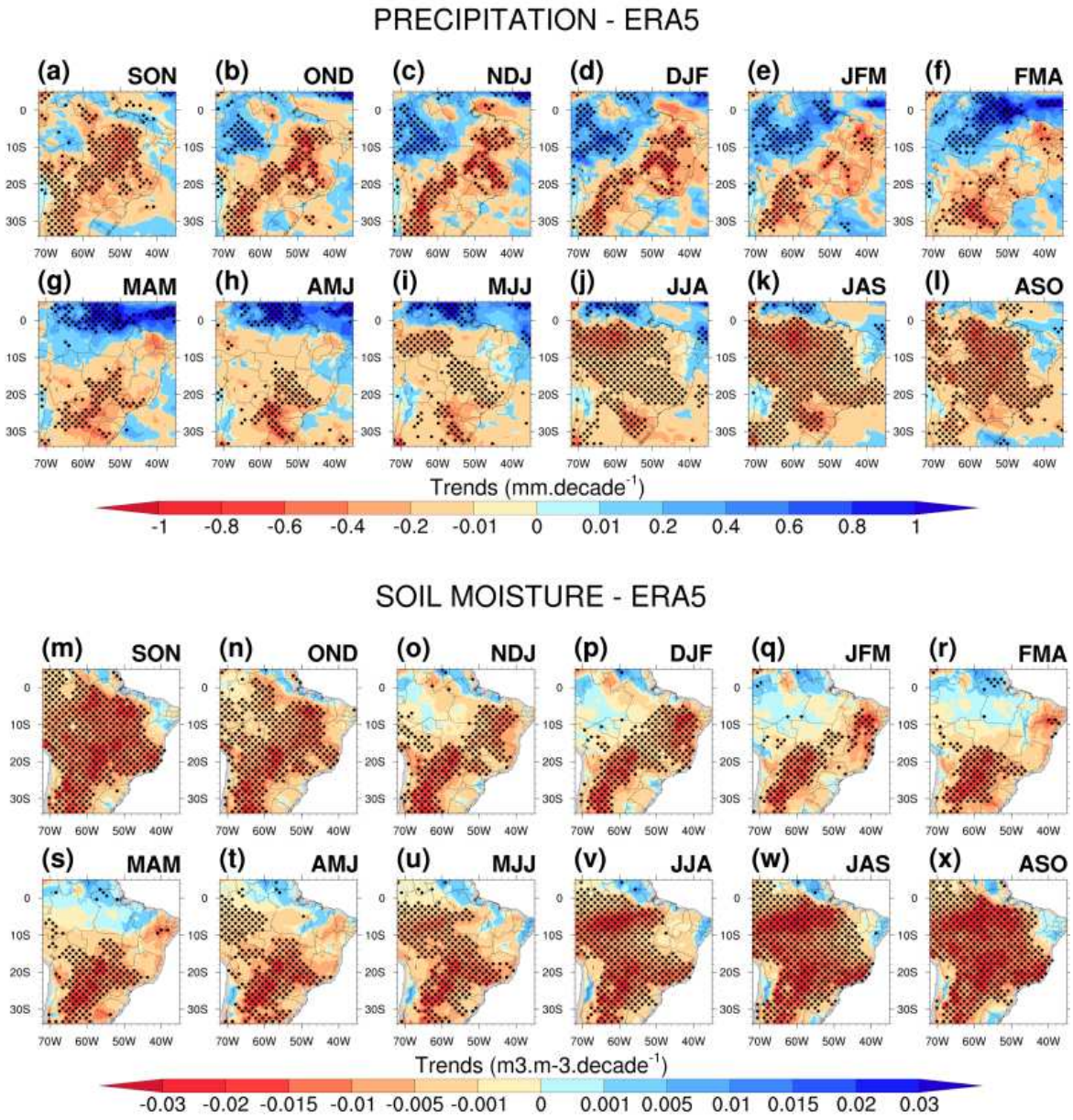

Figure 3: Trends of precipitation and soil moisture in a trimester moving window over South America (1980-2020) from ERA5. Hatched areas represent statistically significant trends at 95%.

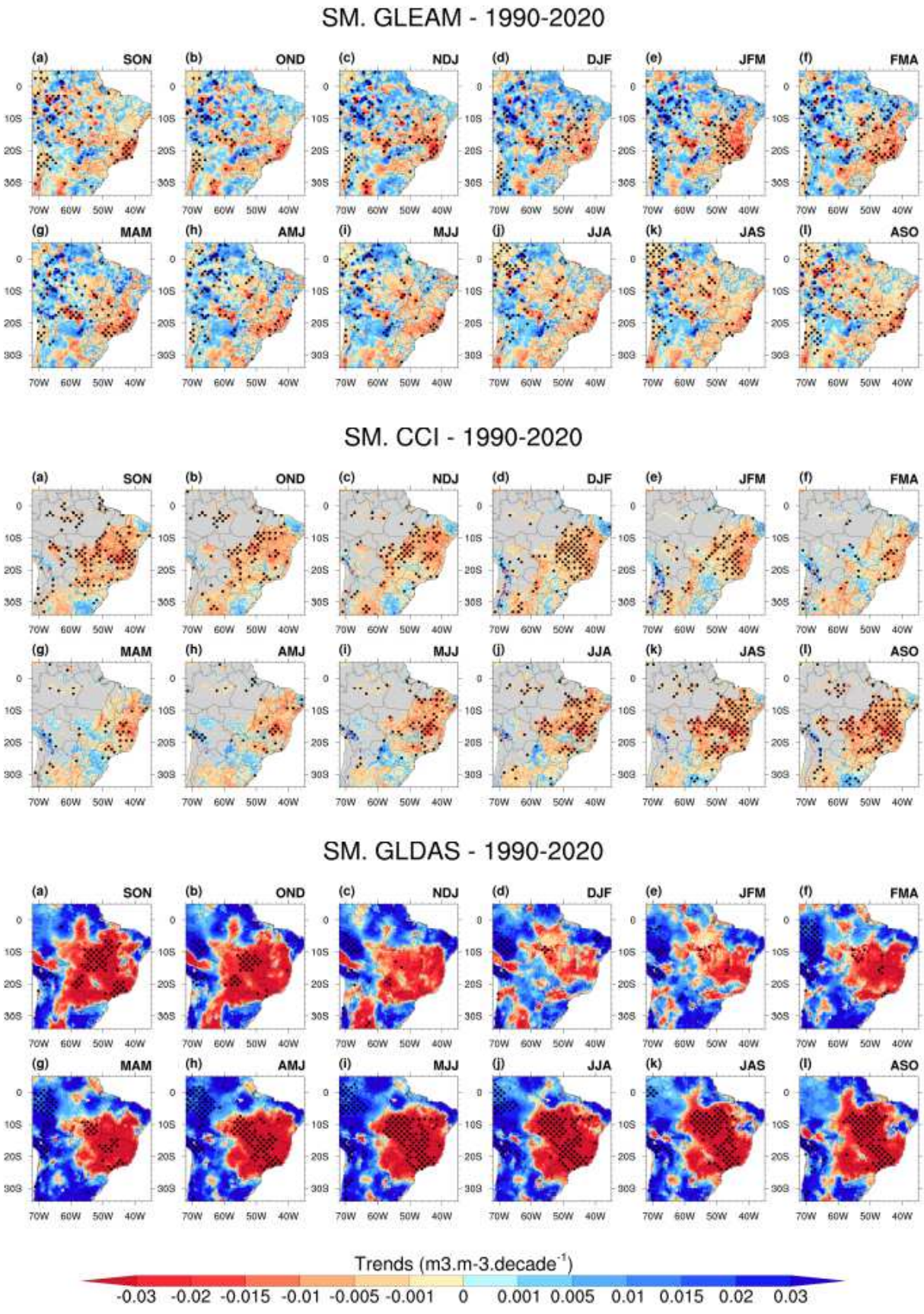

Figure 4: Soil moisture trends for GLEAM, CCI and GLDAS in a trimester moving window. Dots represent statistically significant trends at 95%.

South America's climate is influenced by a variety of dynamic systems that shape regional precipitation and soil moisture trends. The South Atlantic Convergence Zone (SACZ) significantly increases rainfall in the south and southeast during DJF and MAM, while the Intertropical Convergence Zone (ITCZ) enhances precipitation in northern regions. Conversely, the continental expansion of the South Atlantic Subtropical High (SASH) often induces drought conditions in Brazil, particularly during JJA and SON. Cold fronts bring rain to southern Brazil in MAM and JJA, while Upper Tropospheric Cyclonic Vortices (UTCVs) increase precipitation in Northeast Brazil. The Moisture Convergence Zone fosters rising soil moisture and precipitation in central areas, especially in DJF and MAM. Additionally, Easterly Waves contribute to rainfall in Northeast Brazil during MJJ and JJA, and both the Continental and Atlantic Equatorial Masses influence precipitation patterns, with the Atlantic equatorial air mass enhancing moisture in northern and northeastern regions, particularly during DJF and MAM.

Overall, the trends exhibit notable spatial and temporal variability, with certain regions experiencing more pronounced changes. The analysis suggests a direct link between changes in precipitation and soil moisture trends, in particular during the rainy and dry seasons, as regions often display consistent patterns of either increasing or decreasing trends in both variables. This underscores the significant impact of shifting precipitation patterns on soil moisture, which can, in turn, influence hydrology and may pose a threat to population due to increasing frequency and power of extreme events.

3.4 Power Spectrum

To investigate long-term variations in soil moisture, spectral analysis was conducted on the first principal component derived from EOF analysis of each dataset. This analysis aimed to identify dominant frequencies distinct that associated with the seasonal (Fig. 5). The power spectra of soil moisture data from ERA5 and CCI exhibited similar characteristics with minimal peaks, suggesting that these datasets may primarily capture noise and lack prominent periodic components. In contrast, GLEAM and GLDAS data display distinct periodic signals in their power spectra that

exceed the 95\% significance level, with notable peaks observed at frequencies of approximately 0.055 and 0.040 cycles per unit time, which correspond to periods of approximately 18 and 33 months, respectively. These findings suggest that GLEAM and GLDAS may be more sensitive to long$-$term variations in soil moisture, compared to ERA5 and CCI (Fig. 5c,d).

The peak of 0.038 cycles/month in both GLEAM and GLDAS, indicates a consistent periodic signal that may be linked to large-scale climate factors with a biennial cycle. Short-term climate variations may explain the 17-month periodicity in GLEAM, reflecting the complex interaction of climatic and hydrological processes in the region. The GLEAM power spectrum is dominated by a red noise characterization, which is more representative of long-term phenomena, such as SST stochastic model (Hasselman, 1976, Frankignoul and Hasselmann, 1977). Although, it may be speculative to attribute these temporal fluctuations to climate oscillation without further investigations, it has been demonstrated that the Quasi$-$Biennial Oscillation (QBO), with periodicity of approximately 2.2 years, affects precipitation in the tropics, and South America (Garcia-Franco et al., 2022), by changing the monsoonal system (Liess and Geller, 2012), the Intertropical Convergence Zone (ITCZ) (Gray et al., 2018), and tropical sea-surface temperatures (SSTs) (Huang et al., 2012). Moreover, the QBO may interact with the Madden-Julian Oscillation modifying precipitation pattern associated with the SACZ, as discussed by Sena et al., (2022).

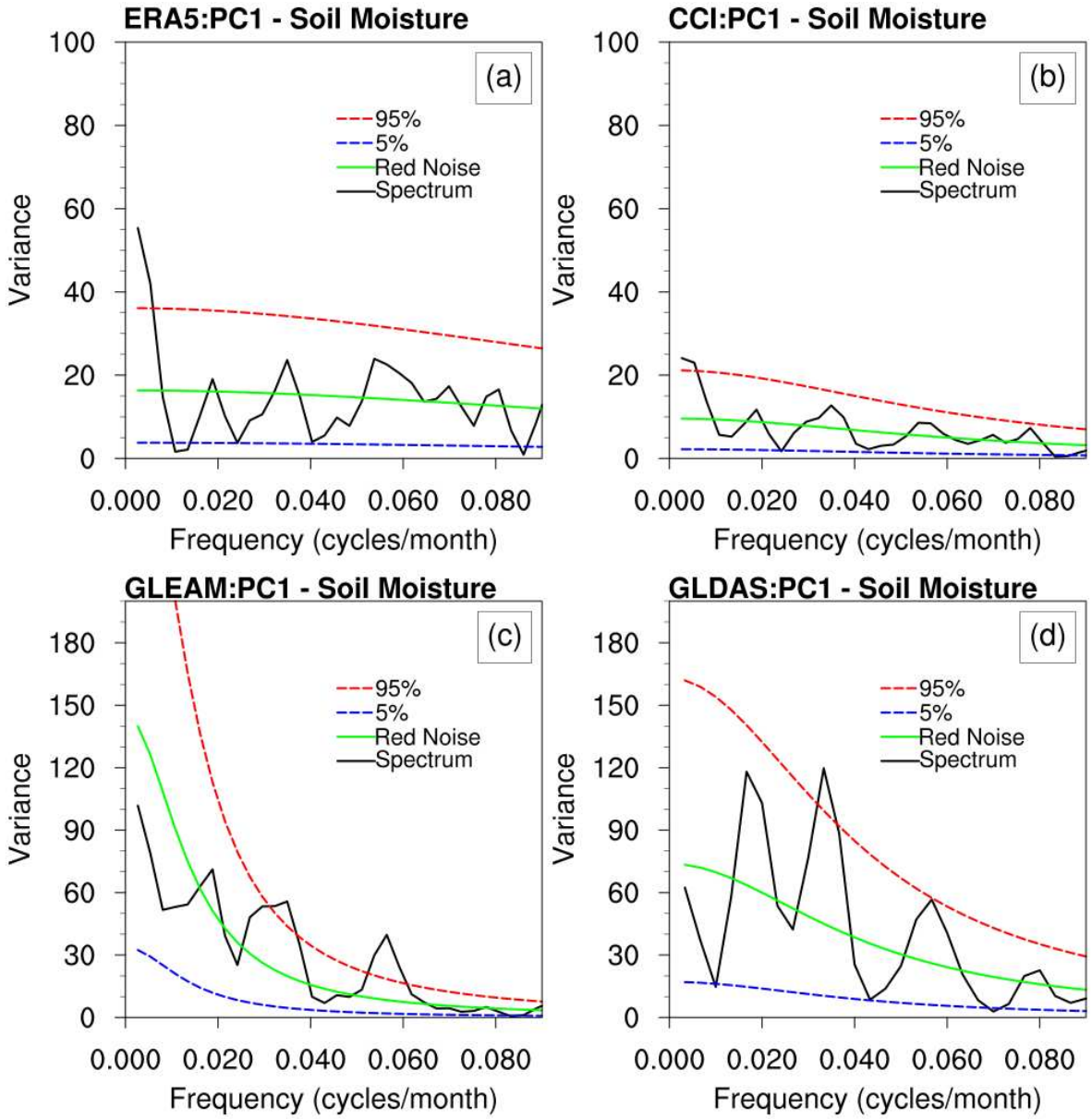

Figure 5: Spectral Analysis of the EOF first principal component of soil moisture datasets (CCI, ERA5, GLDAS, GLEAM).

3.4 Response of SM and precipitation to SAM, ENSO and TAV

Previous spectrum analyses demonstrated that changes in SM may be related to climatic phenomena occurring far from South America or associated with oceanic characteristics in the vicinity of the continent. In this sense, the following analyses aim to identify the response of SM and precipitation to SAM, ENSO and TAV by applying the auto-regressive method.

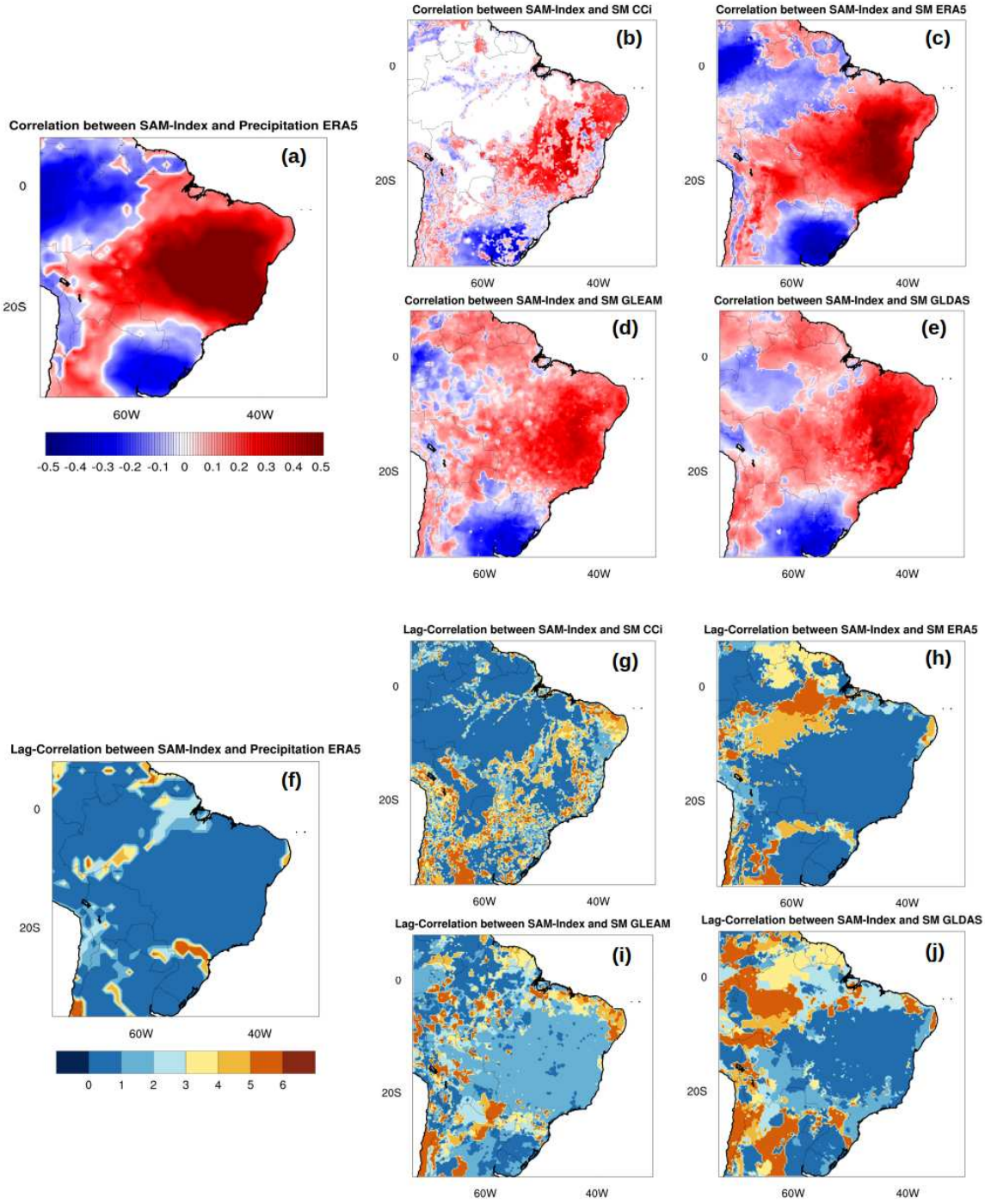

Figure 6: a-e) Maximum correlation between SAM Index and Precipitation (ERA5) / Soil Moisture (CCI, ERA5, GLDAS, GLEAM). f-j) shows the corresponding lag (month) of the maximum correlation.

The influence of the SAM (Fig. 6) on precipitation shows positive correlations across central Brazil, indicating that during monsoonal periods these areas experience more rainfall, as might be expected (Gurjao et al. 2023; Carvalho et al., 2012; Coelho et al., 2022). Conversely, the south and northwestern regions of South America

experience reduced precipitation (Fig. 6a). In fact, the SAM does shift the main region of convection northward resulting in less precipitation in southern South America (Coelho et al., 2022). Across western Amazon, on the other hand, negative correlations may be associated with the strengthening of Pacific Walker Circulation (Lyu et al., 2024).

Correlations between the SAM index and soil moisture datasets (Fig. 6b-e) suggest a general consistency in the positive relationship between the SAM and soil moisture across central and northern Brazil, as observed in CCI and ERA5 (Fig. 6b,c). However, the extent and strength of these correlations varied across datasets, highlighting the importance of considering data source variability when analyzing climate-soil moisture interactions. The weaker contrasting patterns observed in GLDAS and in particular in GLEAM (Fig. 6e,d), between positive and negative correlations may indicate the influence of regional climatic or environmental factors on the soil moisture response to the SAM. It has to be mentioned, moreover, that both datasets may be influenced by parameterization of the land surface model applied to provide soil moisture estimates.

The maximum correlation between the SAM and precipitation occurs at lag 0 across most of South America (Fig. 6f). However, soil moisture shows peak correlations at varying lags. In particular, ERA5 and GLDAS exhibit maximum correlations in northern South America with lags of 3-5 months (Fig. 6h,j), indicating that soil moisture reaches its highest values 3-5 months after the onset of the SAM. GLEAM and CCI display distinct patterns, with CCI dominated by regional small-scale features, while GLEAM primarily responds at a lag of 2 months with respect to the SAM (Fig. 6g,i).

Turning to evaluation of the precipitation response to the TAV, it is interesting to mention that no large differences arise by comparing this result with previously discussed rainfall response to the SAM (Fig. 7a). However, it may be highlighted that the TAV induces lower precipitation/negative correlation, across the Amazon and the northeastern portion of Brazil (Fig. 7a). Regarding the soil moisture response, several differences are noticed among the datasets. It is clear that the SM ERA5 does match

very closely with the precipitation features, which is somehow reproduced also by the CCI and GLEAM (Fig. 7b,d), the former although reproduced small scale features. However, a significant shift occurred in the Amazon/Savanna transition zone, where the region characterized by high positive correlations between TAV and precipitation in the precipitation analysis, exhibited negative correlations in soil moisture. This is more evident in the correlation pattern delivered by the GLDAS, where most of northern South America is characterized by negative correlations and consequently reduced soil moisture (Fig. 7e).

The lag correlation maps provide crucial insights into the timing of the TAV's influence on precipitation and soil moisture (Fig. 7f-j). By mapping the month of maximum correlation (Fig. 7a-e), these maps reveal the phase lag between the TAV index and its impact on these variables. The TAV exerts a significant influence on the climate of South America. In the Amazon Basin, positive TAV phases, associated with warmer-than-average North Atlantic conditions, lead to reduced precipitation within approximately one month. Focusing on central South America, the TAV exerts its primary impact on precipitation with a lag of roughly 3-4 months.

Regarding soil moisture, a general consensus emerges across the Amazon and northern South America, with all datasets indicating a 1-2 month lag response to TAV variations. However, regional discrepancies arise. While ERA5 and CCI exhibit a strong correspondence between precipitation and soil moisture patterns, GLEAM and GLDAS show deviations. Specifically, ERA5 suggests that meridional changes associated with the TAV lead to increased soil moisture with a 3-4 month lag, slightly longer than the 2-3 (4-5) month lag suggested by GLDAS (GLEAM). This analysis highlights the complexity of the TAV's influence on South American climate, with varying responses observed in precipitation and soil moisture across different datasets and regions.

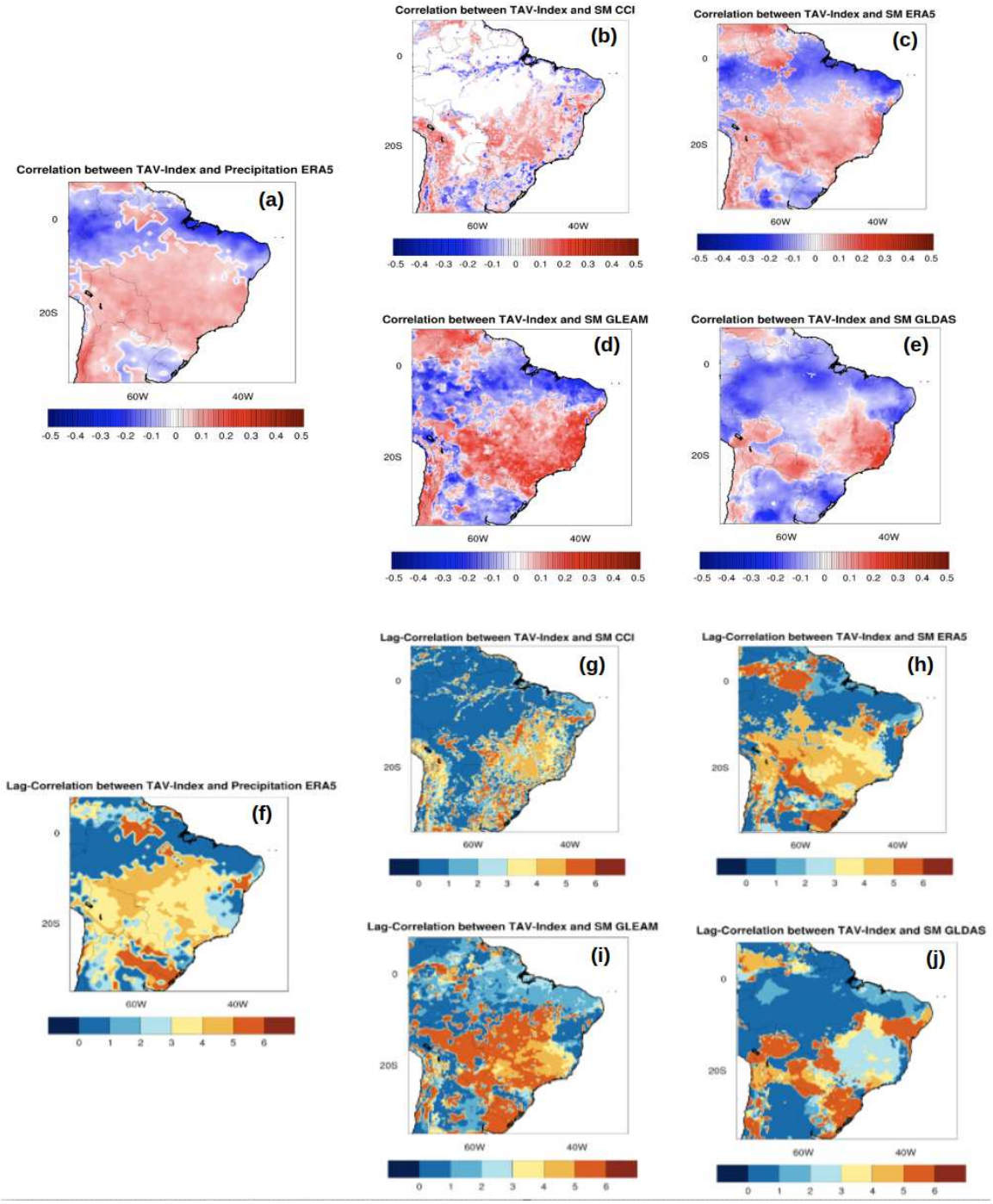

Figure 7. Same as Figure 6 but TAV-Index and Precipitation (ERA5)/Soil Moisture (CCI, ERA5, GLDAS, GLEAM)

The second teleconnection examined in this study focuses on the influence of El Niño-Southern Oscillation (ENSO) on precipitation and, subsequently, soil moisture across South America (Fig. 8a-j). The impact of ENSO on South American precipitation

has been extensively investigated in previous research (Costa et al., 2020; Souza et al., 2021; Bernardino et al., 2017; Kayano et al., 2011, and others) have extensively documented the impact of ENSO on South American precipitation. Main finding indicates that ENSO exerts a significant influence on precipitation patterns across South America. Generally, ENSO events lead to reduced precipitation across much of the continent, while increasing precipitation in southern South America, in agreement with is shown in Figure 8a. Moreover, a notable feature is the strong consonance among soil moisture datasets, indicating a consistent response to ENSO. This response is characterized by a dipole pattern: decreased soil moisture in northern South America (Solander et al., 2020) and increased soil moisture in the southern part of the continent. This dipole is much weaker in the CCI dataset (Fig. 8c).

Turning to the lag correlation maps (Fig. 8f-j), the datasets consistently show that ENSO leads to reductions in precipitation and soil moisture in northeastern Brazil with a lag of 5-6 months. In the Amazon basin and the region between 10°S and 20°S, variations in the response time are evident: ERA5 soil moisture lags ENSO by 2-3 months, while GLEAM and GLDAS exhibit more localized or meso-scale patterns (Fig. 8h-j). South of 20°S, the dominant lag for CCI, GLEAM, and GLDAS extends beyond 5 months, except for ERA5, which responds almost simultaneously to the onset of ENSO (Fig. 8h).

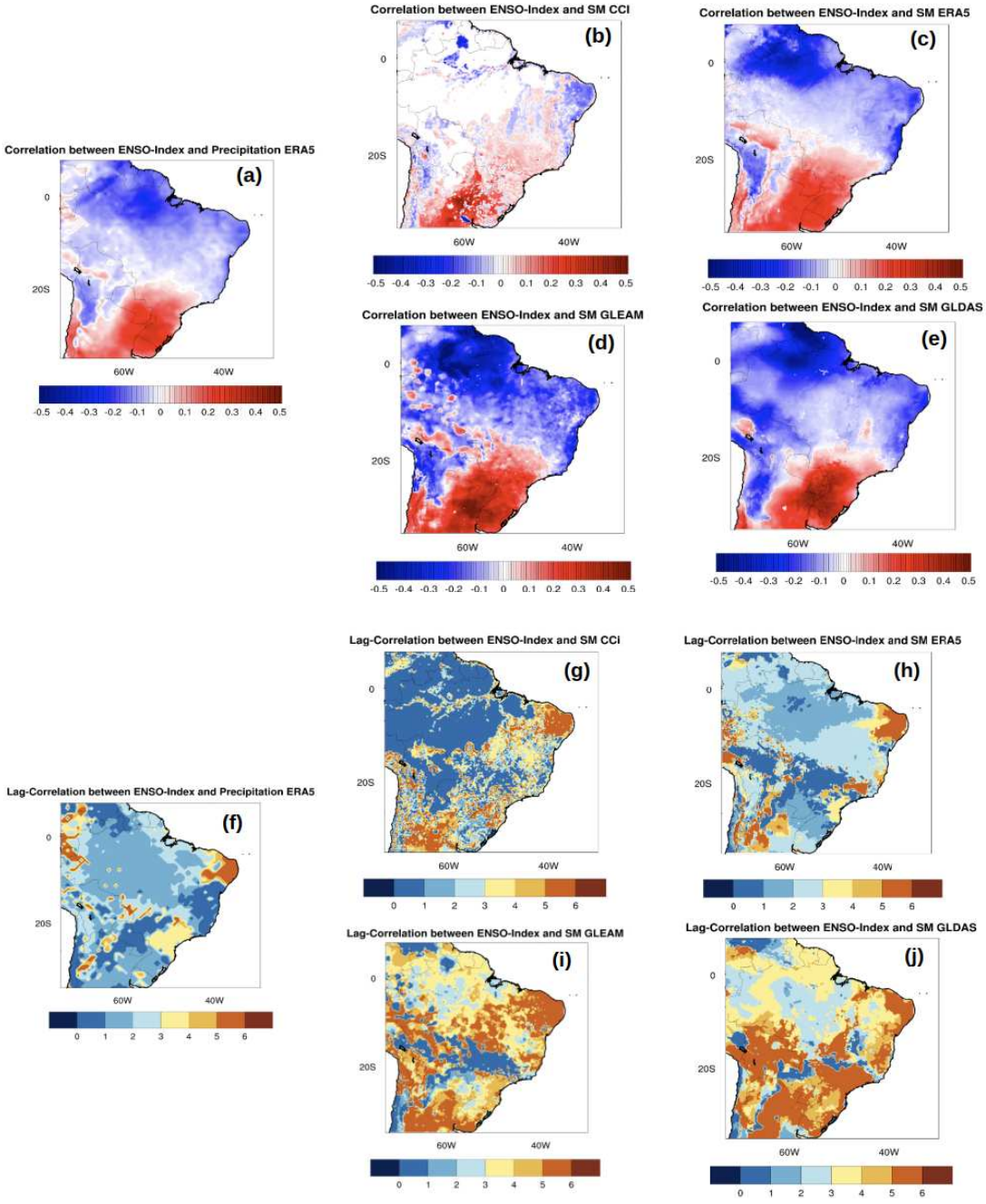

Figure 8: Same as Figure 6 but ENSO-Index and Precipitation (ERA5)/Soil Moisture

4 Concluding remarks

This study presents a comprehensive assessment of soil moisture (SM) variability across South America using four datasets—ERA5, GLEAM, GLDAS, and CCI SM—spanning from January 1990 to December 2020. The results reveal

pronounced regional differences in SM, shaped by diverse climatic systems and environmental drivers.

Trend analysis reveals increasing SM trends in northern South America, consistent with enhanced precipitation over recent decades. In central Brazil, variability is largely governed by the South Atlantic Convergence Zone (SACZ), which drives strong seasonal SM cycles. The central region consistently emerges in EOF patterns as a hotspot of variability, reflecting the SACZ's significant contribution to seasonal SM distribution. Given the region's agricultural importance, these variations are critical, as crop production heavily depends on stable SM conditions.

The spectral and correlation analyses reveal that soil moisture (SM) and precipitation patterns across South America are significantly influenced by large-scale climate modes such as the South America Monsoon (SAM), the Tropical Atlantic Variability (TAV), and the El Niño–Southern Oscillation (ENSO). The SAM shows a strong concurrent impact on precipitation, particularly enhancing rainfall over central Brazil during monsoonal periods, while reducing it in southern and northwestern South America. This response appears linked to shifts in convection zones associated with SAM phases. Soil moisture responses to SAM are more complex, showing notable dataset-dependent variability. While ERA5 and CCI indicate consistent positive correlations in central and northern Brazil, GLDAS and GLEAM reflect weaker and less spatially coherent signals, possibly due to differences in model parameterizations. Additionally, SM responses to SAM often lag precipitation by 2–5 months, underlining the delayed hydrological adjustment of soils.

For the TAV and ENSO, lagged impacts are more prominent and regionally distinct. TAV affects precipitation within a 1–4 month lag, particularly reducing rainfall in the Amazon and northeastern Brazil during its positive phases. Soil moisture responses mirror these rainfall anomalies but also highlight divergent sensitivities across datasets, with ERA5 and CCI more closely reproducing precipitation patterns, while GLDAS and GLEAM present varied lag structures and magnitudes. ENSO exerts a widespread and consistent influence across all datasets, especially in forming a dipole of reduced SM in northern South America and increased SM in the south. The ENSO-related lags in SM responses span from 2 to over 5 months, depending on the region and dataset, indicating the complexity of land–atmosphere interactions. In

general, these findings highlight the importance of considering both the timing and spatial variability of climate–soil moisture relationships, particularly when interpreting impacts of remote teleconnections on regional hydrology. This study demonstrates the value of combining multiple datasets with advanced analytical approaches to capture the complexity of SM variability. Understanding these spatial and temporal patterns is essential for guiding agricultural practices, water management, and climate adaptation. The insights gained here contribute to strategies aimed at mitigating climate change impacts and promoting the long-term socio-economic and environmental sustainability of South America.

References

Arias, P.A., Fu, R., Hoyos, C.D., Li, W. and Zhou, L. (2010). Changes in cloudiness over the Amazon rainforests during the last two decades: diagnostic and potential causes. *Climate Dynamics*, 37(5-6), pp.1151–1164. doi:https://doi.org/10.1007/s00382-010-0903-2.

Arsego, V.B.M., de Gonçalves, L.G.G., Diogo Alessandro , A., Figueroa, S.N., Kubota, P.Y. and de Souza, C.R. (2023). Impact of Soil Moisture in the Monsoon Region of South America during Transition Season. *Atmosphere*, 14(5), pp.804–804. doi:https://doi.org/10.3390/atmos14050804.

Bernardino, B.S., Vasconcellos, F.C. and Nunes, A.M.B. (2017). Impact of the equatorial Pacific and South Atlantic SST anomalies on extremes in austral summer precipitation over Grande river basin in Southeast Brazil. *International Journal of Climatology*, 38, pp.e131–e143. doi:https://doi.org/10.1002/joc.5358.

Carvalho, L.M.V. and Jones, C. (2016). *The Monsoons and Climate Change Observations and Modeling*. Cham Springer International Publishing.

Carvalho, L.M.V., Jones, C., Posadas, A.N.D., Quiroz, R., Bookhagen, B. and Liebmann, B. (2012). Precipitation Characteristics of the South American Monsoon System Derived from Multiple Datasets. *Journal of Climate*, [online] 25(13), pp.4600–4620. doi:https://doi.org/10.1175/jcli-d-11-00335.1.

Chug, D., Dominguez, F. and Yang, Z. (2022). The Amazon and La Plata River Basins as Moisture Sources of South America: Climatology and Intraseasonal Variability. *Journal of Geophysical Research: Atmospheres*, 127(12). doi:https://doi.org/10.1029/2021jd035455.

Coelho, C.A.S., Souza, D.C., Kubota, P.Y., Cavalcanti, I.F.A., Baker, J.C.A., Figueroa, S.N., Firpo, M.A.F., Guimarães, B.S., Costa, S.M.S., Gonçalves, L.J.M., Bonatti, J.P., Sampaio, G., Klingaman, N.P., Chevuturi, A. and Andrews, M.B. (2021).

Assessing the representation of South American monsoon features in Brazil and U.K. climate model simulations. *Climate Resilience and Sustainability*, 1(1). doi:https://doi.org/10.1002/cli2.27.

Collini, E.A., Berbery, E.H., Barros, V.R. and Pyle, M.E. (2008). How Does Soil Moisture Influence the Early Stages of the South American Monsoon? *Journal of Climate*, 21(2), pp.195–213. doi:https://doi.org/10.1175/2007jcli1846.1.

Costa, M. da S., Oliveira-Júnior, J.F. de, Santos, P.J. dos, Correia Filho, W.L.F., Gois, G. de, Blanco, C.J.C., Teodoro, P.E., Silva Junior, C.A. da, Santiago, D. de B., Souza, E. de O. and Jardim, A.M. da R.F. (2020). Rainfall extremes and drought in Northeast Brazil and its relationship with El Niño–Southern Oscillation. *International Journal of Climatology*, 41(S1). doi:https://doi.org/10.1002/joc.6835.

da Silva e Souza, G., Gomes, E.G., Alves, E.R. de A. and Gasques, J.G. (2020). Technological progress in the Brazilian agriculture. *Socio-Economic Planning Sciences*, 72, p.100879. doi:https://doi.org/10.1016/j.seps.2020.100879.

de Souza, I.P., Andreoli, R.V., Kayano, M.T., Vargas, F.F., Cerón, W.L., Martins, J.A., Freitas, E. and Souza, R.A.F. (2021). Seasonal precipitation variability modes over South America associated to El Niño-Southern Oscillation (ENSO) and non-ENSO components during the 1951–2016 period. *International Journal of Climatology*, 41(8), pp.4321–4338. doi:https://doi.org/10.1002/joc.7075.

Dorigo, W.A., Gruber, A., De Jeu, R.A.M., Wagner, W., Stacke, T., Loew, A., Albergel, C., Brocca, L., Chung, D., Parinussa, R.M. and Kidd, R. (2015). Evaluation of the ESA CCI soil moisture product using ground-based observations. *Remote Sensing of Environment*, 162, pp.380–395. doi:https://doi.org/10.1016/j.rse.2014.07.023.

Fang, L., Hain, C.R., Zhan, X. and Anderson, M.C. (2016). An inter-comparison of soil moisture data products from satellite remote sensing and a land surface model. *International Journal of Applied Earth Observation and Geoinformation*, 48, pp.37–50. doi:https://doi.org/10.1016/j.jag.2015.10.006.

FRANKIGNOUL, C. and HASSELMANN, K. (1977). Stochastic climate models, Part II Application to sea-surface temperature anomalies and thermocline variability. *Tellus*, 29(4), pp.289–305. doi:https://doi.org/10.1111/j.2153-3490.1977.tb00740.x.

Furtak, K. and Agnieszka Wolińska (2023). The impact of extreme weather events as a consequence of climate change on the soil moisture and on the quality of the soil environment and agriculture – A review. *Catena*, 231, pp.107378–107378. doi:https://doi.org/10.1016/j.catena.2023.107378.

García-Franco, J.L., Gray, L.J., Osprey, S., Chadwick, R. and Martin, Z. (2022). The tropical route of quasi-biennial oscillation (QBO) teleconnections in a climate model. *Weather and Climate Dynamics*, 3(3), pp.825–844. doi:https://doi.org/10.5194/wcd-3-825-2022.

Gouveia, C.M., Justino, F., Gurjao, C., Zita, L. and Alonso, C. (2023). Revisiting Climate-Related Agricultural Losses across South America and Their Future

Perspectives. *Atmosphere*, [online] 14(8), p.1303. doi:https://doi.org/10.3390/atmos14081303.

Gray, L.J., Anstey, J.A., Kawatani, Y., Lu, H., Osprey, S. and Schenzinger, V. (2018). Surface impacts of the Quasi Biennial Oscillation. *Atmospheric Chemistry and Physics*, 18(11), pp.8227–8247. doi:https://doi.org/10.5194/acp-18-8227-2018.

Guo, Z., Dirmeyer, P.A., Hu, Z.-Z., Gao, X. and Zhao, M. (2006). Evaluation of the Second Global Soil Wetness Project soil moisture simulations: 2. Sensitivity to external meteorological forcing. *Journal of Geophysical Research*, 111(D22). doi:https://doi.org/10.1029/2006jd007845.

Guo, Z., Li, X., Ren, Y., Qian, S. and Shao, Y. (2023). Research on regional soil moisture dynamics based on hyperspectral remote sensing technology. *The international journal of low carbon technologies*, 18, pp.737–749. doi:https://doi.org/10.1093/ijlct/ctad051.

Gurjão, C., Justino, F., Pires, G., Senna, M., Lindemann, D. and Rodrigues, J. (2023). Southern hemisphere monsoonal system during superinterglacial stages: MIS5e, MIS11c and MIS31. *Climate Dynamics*, 61(3-4), pp.1867–1885. doi:https://doi.org/10.1007/s00382-023-06660-7.

Hasselmann, K. (1976). Stochastic climate models Part I. Theory. *Tellus*, 28(6), pp.473–485. doi:https://doi.org/10.1111/j.2153-3490.1976.tb00696.x.

Hersbach, H., Bell, B., Berrisford, P., Hirahara, S., Horányi, A., Muñoz-Sabater, J., Nicolas, J., Peubey, C., Radu, R., Schepers, D., Simmons, A., Soci, C., Abdalla, S., Abellan, X., Balsamo, G., Bechtold, P., Biavati, G., Bidlot, J., Bonavita, M. and Chiara, G. (2020). The ERA5 global reanalysis. *Quarterly Journal of the Royal Meteorological Society*, 146(730). doi:https://doi.org/10.1002/qj.3803.

Huang, B., Hu, Z.-Z., Kinter, J.L., Wu, Z. and Kumar, A. (2011). Connection of stratospheric QBO with global atmospheric general circulation and tropical SST. Part I: methodology and composite life cycle. *Climate Dynamics*, 38(1-2), pp.1–23. doi:https://doi.org/10.1007/s00382-011-1250-7.

Jiang, J., Liu, Y., Mao, J. and Wu, G. (2023). Extreme heatwave over Eastern China in summer 2022: the role of three oceans and local soil moisture feedback. *Environmental Research Letters*, 18(4), pp.044025–044025. doi:https://doi.org/10.1088/1748-9326/acc5fb.

Jiang, K., Pan, Z., Pan, F., Wang, J., Han, G., Song, Y., Zhang, Z., Huang, N., Ma, S. and Chen, X. (2022). Influence patterns of soil moisture change on surface-air temperature difference under different climatic background. *Science of The Total Environment*, 822, p.153607. doi:https://doi.org/10.1016/j.scitotenv.2022.153607.

Jucá, M.V.Q. and Neto, A.R. (2022). Remote sensing and global databases for soil moisture estimation at different depths in the Pernambuco state, Northeast Brazil. *RBRH*, [online] 27. doi:https://doi.org/10.1590/2318-0331.272220220016.

Kay, G., Dunstone, N.J., Smith, D.M., Betts, R.A., Cunningham, C. and Scaife, A.A. (2022). Assessing the chance of unprecedented dry conditions over North Brazil

during El Niño events. *Environmental Research Letters*, 17(6), p.064016. doi:https://doi.org/10.1088/1748-9326/ac6df9.

Kayano, M.T., Andreoli, R.V. and de Souza, R.A.F. (2011). Evolving anomalous SST patterns leading to ENSO extremes: relations between the tropical Pacific and Atlantic Oceans and the influence on the South American rainfall. *International Journal of Climatology*, 31(8), pp.1119–1134. doi:https://doi.org/10.1002/joc.2135.

Liess, S. and Geller, M.A. (2012). On the relationship between QBO and distribution of tropical deep convection. *Journal of Geophysical Research: Atmospheres*, 117(D3), p.n/a-n/a. doi:https://doi.org/10.1029/2011jd016317.

Lóczy, D., József Dezső, D., Weidinger, T., László Horváth, D., Pirkhoffer, E. and Czigány, S. (2024). Soil Moisture Conservation through Crop Diversification and Related Ecosystem Services in a Blown-Sand Area with High Drought Hazard. *Plants*, [online] 13(4), pp.494–494. doi:https://doi.org/10.3390/plants13040494.

Lornezhad, E., Ebrahimi, H. and Rabieifar, H.R. (2023). Analysis of precipitation and drought trends by a modified Mann–Kendall method: a case study of Lorestan province, Iran. *Water Science & Technology Water Supply*, 23(4), pp.1557–1570. doi:https://doi.org/10.2166/ws.2023.068.

Lü, J., Wang, G., Chen, T., Li, S., Fiifi, D., Giri Kattel, Peng, J., Jiang, T. and Su, B. (2021). A harmonized global land evaporation dataset from model-based products covering 1980–2017. *Earth System Science Data*, 13(12), pp.5879–5898. doi:https://doi.org/10.5194/essd-13-5879-2021.

Lyu, Z., Vuille, M., Goosse, H., Orrison, R., Novello, V.F., Cruz, F.W., Stríkis, N.M. and Cauhy, J. (2024). South American monsoon intensification during the last millennium driven by joint Pacific and Atlantic forcing. *Science Advances*, 10(38). doi:https://doi.org/10.1126/sciadv.ado9543.

Marengo, J.A. (2009). Long-term trends and cycles in the hydrometeorology of the Amazon basin since the late 1920s. *Hydrological Processes*, 23(22), pp.3236–3244. doi:https://doi.org/10.1002/hyp.7396.

Marengo, J.A. and Espinoza, J.C. (2015). Extreme seasonal droughts and floods in Amazonia: causes, trends and impacts. *International Journal of Climatology*, 36(3), pp.1033–1050. doi:https://doi.org/10.1002/joc.4420.

Martens, B., Miralles, D.G., Lievens, H., van der Schalie, R., de Jeu, R.A.M., Fernández-Prieto, D., Beck, H.E., Dorigo, W.A. and Verhoest, N.E.C. (2017). GLEAM v3: satellite-based land evaporation and root-zone soil moisture. *Geoscientific Model Development*, 10(5), pp.1903–1925. doi:https://doi.org/10.5194/gmd-10-1903-2017.

Mohseni, F., Jamali, S., Arsalan Ghorbanian and Mehdi Mokhtarzade (2023). Global soil moisture trend analysis using microwave remote sensing data and an automated polynomial-based algorithm. *Global and Planetary Change*, 231, pp.104310–104310. doi:https://doi.org/10.1016/j.gloplacha.2023.104310.

Nielsen, D.M., Cataldi, M., Belém, A.L. and Albuquerque, A.L.S. (2016). Local indices for the South American monsoon system and its impacts on Southeast Brazilian

precipitation patterns. *Natural Hazards*, 83(2), pp.909–928. doi:https://doi.org/10.1007/s11069-016-2355-4.

O'Donnell, M.S. and Manier, D.J. (2022). Spatial Estimates of Soil Moisture for Understanding Ecological Potential and Risk: A Case Study for Arid and Semi-Arid Ecosystems. *Land*, [online] 11(10), p.1856. doi:https://doi.org/10.3390/land11101856.

Park, J.-H. and Li, T. (2018). Interdecadal modulation of El Niño–tropical North Atlantic teleconnection by the Atlantic multi-decadal oscillation. *Climate Dynamics*, 52(9-10), pp.5345–5360. doi:https://doi.org/10.1007/s00382-018-4452-4.

Qin, T., Feng, J., Zhang, X., Li, C., Fan, J., Zhang, C., Dong, B., Wang, H. and Yan, D. (2023). Continued decline of global soil moisture content, with obvious soil stratification and regional difference. *Science of The Total Environment*, [online] 864, p.160982. doi:https://doi.org/10.1016/j.scitotenv.2022.160982.

Rasheed, M.W., Tang, J., Sarwar, A., Shah, S., Saddique, N., Khan, M.U., Imran Khan, M., Nawaz, S., Shamshiri, R.R., Aziz, M. and Sultan, M. (2022). Soil Moisture Measuring Techniques and Factors Affecting the Moisture Dynamics: A Comprehensive Review. *Sustainability*, 14(18), p.11538. doi:https://doi.org/10.3390/su141811538.

Rodrigues, R.R. and McPhaden, M.J. (2014). Why did the 2011-2012 La Niña cause a severe drought in the Brazilian Northeast? *Geophysical Research Letters*, 41(3), pp.1012–1018. doi:https://doi.org/10.1002/2013gl058703.

Santos, M.J., Silva Dias, M.A.F. and Freitas, E.D. (2014). Influence of local circulations on wind, moisture, and precipitation close to Manaus City, Amazon Region, Brazil. *Journal of Geophysical Research: Atmospheres*, 119(23), pp.13, 233–13, 249. doi:https://doi.org/10.1002/2014jd021969.

Santos, T.V., De Freitas, L.D.A., Gonçalves, R.D. and Chang, H.K. (2020). Teste de Mann-Kendall aplicado à dados hidrológicos – Desempenho dos filtros TFPW e CV2 na análise de tendências. *Ciência e Natura*, 42, p.e87. doi:https://doi.org/10.5902/2179460x41928.

Sehler, R., Li, J., Reager, J. and Ye, H. (2019). Investigating Relationship Between Soil Moisture and Precipitation Globally Using Remote Sensing Observations. *Journal of Contemporary Water Research & Education*, 168(1), pp.106–118. doi:https://doi.org/10.1111/j.1936-704x.2019.03324.x.

Sena, A.C.T., Peings, Y. and Magnusdottir, G. (2022). Effect of the Quasi-Biennial Oscillation on the Madden Julian Oscillation Teleconnections in the Southern Hemisphere. *Geophysical Research Letters*, 49(6). doi:https://doi.org/10.1029/2021gl096105.

Skendžić, S., Zovko, M., Živković, I.P., Lešić, V. and Lemić, D. (2021). The Impact of Climate Change on Agricultural Insect Pests. *Insects*, 12(5), p.440. doi:https://doi.org/10.3390/insects12050440.

Solander, K.C., Newman, B.D., Carioca de Araujo, A., Barnard, H.R., Berry, Z.C., Bonal, D., Bretfeld, M., Burban, B., Antonio Candido, L., Célleri, R., Chambers, J.Q.,

Christoffersen, B.O., Detto, M., Dorigo, W.A., Ewers, B.E., José Filgueiras Ferreira, S., Knohl, A., Leung, L.R., McDowell, N.G. and Miller, G.R. (2020). The pantropical response of soil moisture to El Niño. *Hydrology and Earth System Sciences*, [online] 24(5), pp.2303–2322. doi:https://doi.org/10.5194/hess-24-2303-2020.

Song, H., Tian, J., Huang, J., Guo, P., Zhang, Z. and Wang, J. (2019). Hybrid Causality Analysis of ENSO's Global Impacts on Climate Variables Based on Data-Driven Analytics and Climate Model Simulation. *Frontiers in Earth Science*, 7. doi:https://doi.org/10.3389/feart.2019.00233.

Spennemann, P.C., Rivera, J.A., Saulo, A.C. and Penalba, O.C. (2015). A Comparison of GLDAS Soil Moisture Anomalies against Standardized Precipitation Index and Multisatellite Estimations over South America. *Journal of Hydrometeorology*, 16(1), pp.158–171. doi:https://doi.org/10.1175/jhm-d-13-0190.1.

Thompson, V., Kennedy-Asser, A.T., Vosper, E., Lo, Y.T.E., Huntingford, C., Andrews, O., Collins, M., Hegerl, G.C. and Mitchell, D. (2022). The 2021 western North America heat wave among the most extreme events ever recorded globally. *Science Advances*, 8(18). doi:https://doi.org/10.1126/sciadv.abm6860.

Upadhyay, S. and Raghubanshi, A.S. (2020). Determinants of soil carbon dynamics in urban ecosystems. *Urban Ecology*, pp.299–314. doi:https://doi.org/10.1016/b978-0-12-820730-7.00016-1.

Utida, G., Cruz, F.W., Etourneau, J., Bouloubassi, I., Schefuß, E., Vuille, M., Novello, V.F., Prado, L.F., Sifeddine, A., Klein, V., Zular, A., Viana, J.C.C. and Turcq, B. (2019). Tropical South Atlantic influence on Northeastern Brazil precipitation and ITCZ displacement during the past 2300 years. *Scientific Reports*, 9(1). doi:https://doi.org/10.1038/s41598-018-38003-6.

Walne, C.H. and Reddy, K.R. (2021). Developing Functional Relationships between Soil Waterlogging and Corn Shoot and Root Growth and Development. *Plants*, [online] 10(10), p.2095. doi:https://doi.org/10.3390/plants10102095.

Wang, T., Franz, T.E., Li, R., You, J., Shulski, M.D. and Ray, C. (2017). Evaluating climate and soil effects on regional soil moisture spatial variability using EOFs. *Water Resources Research*, 53(5), pp.4022–4035. doi:https://doi.org/10.1002/2017wr020642.

Xu, H. and Deng, Y. (2018). Dependent Evidence Combination Based on Shearman Coefficient and Pearson Coefficient. *IEEE Access*, 6, pp.11634–11640. doi:https://doi.org/10.1109/access.2017.2783320.

Yang, T., Ala, M., Zhang, Y., Wu, J., Wang, A. and Guan, D. (2018). Characteristics of soil moisture under different vegetation coverage in Horqin Sandy Land, northern China. *PLOS ONE*, 13(6), p.e0198805. doi:https://doi.org/10.1371/journal.pone.0198805.

Yue, W., Meng, K., Hou, K., Zuo, R., Zhang, B.-T. and Wang, G. (2020). Evaluating climate and irrigation effects on spatiotemporal variabilities of regional groundwater in an arid area using EOFs. *The Science of The Total Environment*, 709, pp.136147–136147. doi:https://doi.org/10.1016/j.scitotenv.2019.136147.

Zeng, Y., Zhou, Z., Yan, Z., Teng, M. and Huang, C. (2019). Climate Change and Its Attribution in Three Gorges Reservoir Area, China. *Sustainability*, 11(24), p.7206. doi:https://doi.org/10.3390/su11247206.

Zhang, Z., Pan, Z., Pan, F., Zhang, J., Han, G., Huang, N., Wang, J., Pan, Y., Wang, Z. and Peng, R. (2020). The Change Characteristics and Interactions of Soil Moisture and Temperature in the Farmland in Wuchuan County, Inner Mongolia, China. *Atmosphere*, 11(5), p.503. doi:https://doi.org/10.3390/atmos11050503.

Artigo 2: South America Moisture Fluxes Responses to Atlantic and Pacific Ocean and Implications for the Incidence of Fire Outbreaks

Abstract

The Cerrado region of Brazil is a critical ecological and agricultural zone highly dependent on atmospheric moisture fluxes from the Amazon Basin, Atlantic Ocean, and Pacific Ocean. This study investigates the influence of these moisture sources on precipitation variability and their implications for fire outbreaks. Using the 2L-DRM model and reanalysis datasets, we quantify the contributions of different moisture sources and analyze their response to large-scale climate variability, particularly ENSO and TAV. Results show that Amazonian and Atlantic moisture dominate precipitation in the Cerrado, especially during the wet season, with the SACZ playing a crucial role in moisture transport. El Niño weakens Amazonian moisture transport and shifts SACZ patterns, leading to drier conditions and increased fire risk, whereas La Niña enhances moisture availability, reducing fire susceptibility. EOF analysis highlights seasonal shifts in moisture fluxes, with Amazonian and Atlantic contributions prevailing in summer, while winter exhibits significantly reduced transport, reinforcing drought conditions. The lag correlation analysis indicates that moisture flux variations influence fire activity with a delay, highlighting the need for early warning systems. This study underscores the importance of Amazon conservation and land-use management to mitigate fire risks and maintain sustainable water resources in central Brazil.

1 Introduction

The central region of Brazil, particularly the Cerrado, is a vital ecological and agricultural zone, often referred to as the "breadbasket" of the country due to its significant contributions to Brazil's agricultural output. This region's climate and hydrology are critical to sustaining both its biodiversity and agricultural productivity (Rodrigues et al., 2022). However, the Cerrado and surrounding areas are increasingly vulnerable to environmental changes, particularly those driven by variations in moisture fluxes from the Atlantic and Pacific Oceans (He et al., 2021). These fluxes not only influence precipitation patterns but can also play a crucial role in shaping the

frequency and intensity of fire events, which pose significant threats to both natural ecosystems and agricultural activities (Senande-Rivera et al., 2025).

The Cerrado is characterized by a distinct wet and dry season (Pereira Júnior et al. 2014), with moisture transport from the ocean basins and Amazon being a key driver of this seasonal variability. Changes in the intensity and direction of these moisture fluxes can lead to significant alterations in the region's hydrological cycle, impacting soil moisture levels, vegetation health, and ultimately the susceptibility to fires (Ficklin et al., 2022). While fire remains a natural component of the Cerrado ecosystem, its increasing frequency and intensity are largely attributed to anthropogenic activities such as deforestation, land conversion for agriculture, and the widespread use of fire as a land management tool (Oliveira et al., 2022; Schmidt & Eloy, 2020).

Climate change has further exacerbated fire risk in the Cerrado. Rising temperatures and prolonged dry spells have increased evapotranspiration rates, leading to a more flammable environment (Feron et al., 2019). Moreover, shifts in large-scale climate patterns, such as Atlantic and Pacific multidecadal variability, impact the precipitation in the region. These changes can have a great impact specially when both are in cold phases and reduce the precipitation during winter, making wildfire events more frequent and severe (He et al., 2021).

Beyond climatic factors, land-use changes have played a critical role in intensifying fire activity in the Cerrado. The expansion of agriculture and pasturelands has reduced natural firebreaks and increased the accumulation of combustible vegetation, such as dry grasses and crop residues (Arruda et al., 2024). Fire is frequently used to clear land, but inadequate control measures often result in wildfires that spread uncontrollably, damaging natural ecosystems and agricultural fields (Pivello et al., 2021). Furthermore, deforestation in the Amazon has disrupted regional moisture fluxes, reducing atmospheric humidity transport into central Brazil, which in turn exacerbates drought conditions and increases fire vulnerability (Hofmann et al., 2023). These interlinked processes highlight the urgent need for comprehensive fire management strategies that integrate climate projections, sustainable land-use practices, and improved monitoring systems to mitigate fire risks in the Cerrado.

Moisture flux studies in the Cerrado are essential for understanding regional hydrological cycles and climate variability, given the Cerrado's strategic location between the Amazon, Atlantic Ocean, and other moisture sources. Studies have shown that the Amazon Basin plays a crucial role in supplying atmospheric moisture to the Cerrado through moisture recycling and transport mechanisms, largely governed by the South American Monsoon System (SAMS) (Silva and Kousky, 2012). Besides, the known “Flying rivers” that transport a great volume of atmospheric moisture from the forest to other parts of Brazil, passing over the Andes (Arraut et al., 2012). The South Atlantic Convergence Zone (SACZ) is another major influence, channeling moisture from the Atlantic Ocean and southeastern Brazil into the interior regions. These fluxes vary seasonally, with the rainy season (DJF) dominated by moisture advection from the Amazon and Atlantic, while the dry season (JJA) sees a sharp reduction in fluxes, often exacerbating drought conditions (Nobre et al., 2024). Studies employing reanalysis datasets, remote sensing, and climate models have been instrumental in quantifying these fluxes and assessing how they respond to interannual variability and large-scale climate drivers such as ENSO (El Niño-Southern Oscillation) and Tropical Atlantic Variability (TAV) (Marengo et al., 2022; Hofmann et al., 2023; Wong et al., 2021; Cattelan et al., 2024).

Recent research has highlighted the growing impact of land-use changes and deforestation on moisture flux dynamics in the Cerrado, particularly the conversion of native vegetation into croplands and pastures (Cerri et al., 2018; Ribeiro et al., 2024). Deforestation in the Amazon has been linked to reduced evapotranspiration, leading to a decline in moisture transport to the Cerrado, potentially disrupting regional rainfall patterns (Marengo et al., 2022). Additionally, shifts in large-scale circulation patterns, such as a weakening SACZ or changes in the positioning of the Intertropical Convergence Zone (ITCZ), could further influence moisture availability in the region (He et al., 2021). As climate change progresses, extreme events such as prolonged droughts and intense precipitation episodes are expected to alter the hydrological balance in the Cerrado, impacting water resources, agriculture, and biodiversity. Future studies integrating high-resolution modeling, long-term observational data, and improved moisture tracking methodologies will be crucial for predicting how these fluxes evolve under a changing climate and what adaptation strategies may be necessary to mitigate potential water scarcity issues.

To better understand the complex interactions between moisture fluxes, hydrological processes, and fire dynamics in central Brazil, we utilize the 2-layer dynamic recycling model (2L-DRM). The 2L-DRM provides a framework for analyzing how moisture from the Atlantic and Pacific Oceans and the continent are transported and recycled within the region. By incorporating both vertical and horizontal moisture transport (Dominguez et al., 2020), this model allows for a more comprehensive assessment of how oceanic moisture influences regional precipitation and its downstream effects on agriculture and fire risk.

The objectives of this study are to quantify the contributions of Atlantic and Pacific, Amazon, Southeast and other regions of South America moisture fluxes to the hydrological cycle in central Brazil, evaluate how ENSO and TAV events impact these fluxes, and verify whether these events influence fires dynamics in the region. By addressing these goals, this research adds to provide insights crucial for developing strategies to mitigate the impacts of climate variability on fire risk in central west Brazil.

2 Methodology

This study employed a combination of reanalysis datasets, model simulations, and statistical techniques to investigate moisture flux variability and its relationship to fire activity in central South America. We used the 2-Layer Dynamic Recycling Model (2L-DRM) to estimate moisture transport from key sources: the Atlantic Ocean, Pacific Ocean, and the Amazon Basin. The 2L-DRM accounts for moisture uptake and loss across multiple atmospheric layers and allows for the decomposition of moisture contributions to precipitation in a target region.

Meteorological variables were obtained from the ERA5 reanalysis dataset at a spatial resolution of 0.25° × 0.25°, with 6-hour temporal intervals. We also used GLEAM and GLDAS data for soil moisture validation and comparison. The Fire Radiative Power (FRP) data were retrieved from MODIS products (MOD14A1/MYD14A1), aggregated to monthly means.

Moisture fluxes were computed as the integrated water vapor transport (IWVT) in zonal and meridional components. Precipitable water values were extracted for the

Cerrado region using Google Earth Engine and validated against 2L-DRM outputs. Moisture contribution from each basin was expressed in millimeters and analyzed seasonally (DJF, MAM, JJA, SON).

Trend analysis was performed using the non-parametric Mann-Kendall test and Sen's slope estimator to identify significant changes in moisture transport and FRP over time. Pearson and lagged correlations were applied to evaluate lead-lag relationships between moisture variability and fire peaks.

Empirical Orthogonal Function (EOF) analysis was conducted on seasonal and annual moisture flux fields to identify dominant modes of variability. The EOFs were calculated over a spatial domain encompassing the Atlantic, Amazon, and Pacific source regions. We used standardized anomalies to ensure comparability across variables. The first two EOF modes typically explained over 70% of the total variance, with spatial loadings indicating the dominant direction of moisture transport and associated temporal patterns.

2.1 Data

Our study domain compresses the coordinates: 56.4°W - 46.9°W, 10°S - 19.75°S (States: Mato Grosso, Tocantins, Goiás, Minas Gerais, and Mato Grosso do Sul) (Fig. 1). The total area that the moisture fluxes were analyzed compress the coordinates: -110W - 10E, 10N - -40S.

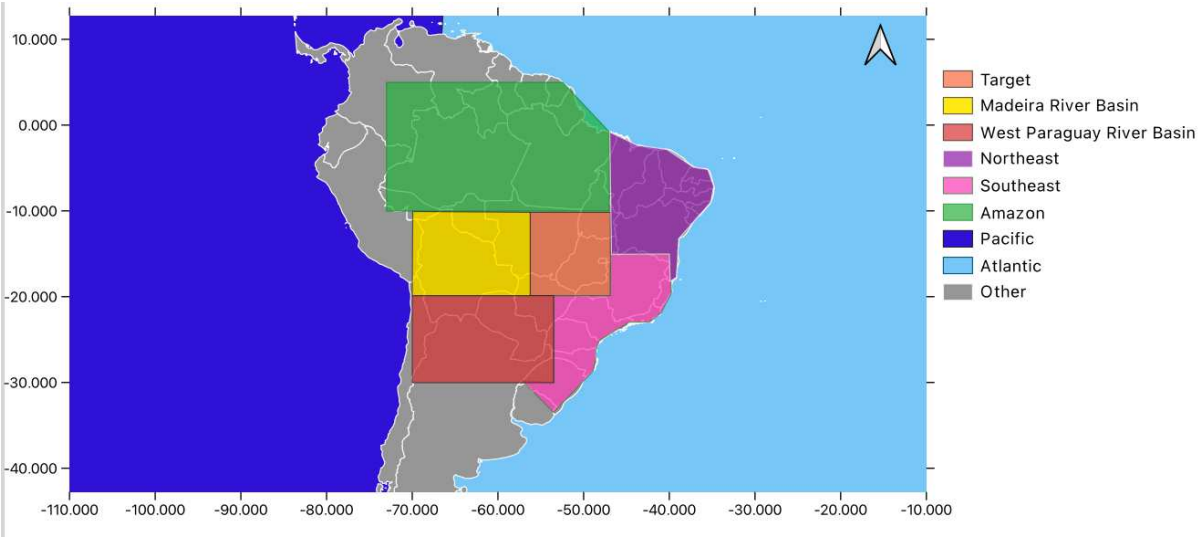

Fig. 1: The domain and five subregions used in this study. It was divided into the target region (Cerrado), Madeira River Basin, West Paraguay River Basin, Northeast, Southeast, Amazon, Pacific and Atlantic oceans and the remaining areas are considered “Others”.

2.2 2L-DRM

In this study, we employed the 2-Layer Dynamical Recycling Model (2L-DRM) to quantify the contribution of different moisture source regions to precipitation in the target area. The 2L-DRM is a simple analytical model that tracks moisture in a semi-Lagrangian framework, this model estimates atmospheric moisture transport by considering the vertical distribution of moisture in two layers of the atmosphere: the upper and lower layers (Dominguez et al., 2020). This approach allows for a more detailed representation of moisture recycling processes compared to single-layer models like the original one-layer DRM, but at the same time it has a lower computational cost of running compared to complex models such as Weather Research and Forecasting regional climate model (WRF-WVT) (Dominguez et al., 2020; Kim and Dominguez, 2023). Besides, complex models are more suitable for capturing individual local-scale processes, because of their precision, therefore 2L-DRM is preferred for studying large-scale processes, such as the focus of our study (Kim and Dominguez, 2023).

The 2L-DRM is based on the conservation of water vapor within an air column, which can be expressed as:

$$P - E = -\frac{1}{g\rho_w}\frac{\partial}{\partial t}\int_0^{p_s} \mathrm{qdp} - \frac{1}{g\rho_w}\frac{\partial}{\partial t}\int_0^{p_s} \nabla.(\widehat{qu})\mathrm{dp} - \frac{1}{g\rho_w} q_s \widehat{u_s} \nabla ps \quad (1)$$

Where:

P is precipitation,

E is evapotranspiration,

g is the Earth's gravitational constant,

ρ_w is the density of water,

q is specific humidity, and

$\hat{u}$is the horizontal wind vector ($\hat{u} = (\hat{u}, \hat{v})$).

Using 3-hourly ERA5 data, vertically integrated water vapor W and moisture-weighted wind components (u, v) were obtained for upper and lower layers.

$$w = \int_{p\ bottom}^{p\ top} q\frac{dp}{g},\ u = \frac{1}{w}\int_{p\ bottom}^{p\ top} q\hat{u}\frac{dp}{g},\ v = \frac{1}{w}\int_{p\ bottom}^{p\ top} q\hat{v}\frac{dp}{g} \quad (2)$$

with p_{top} and p_{bottom}being top and bottom of the slab.

The model provides prognostic equations for the recycling ratio (ρ) in each layer:

$$\frac{dp_1}{dt} = \frac{E(1-\rho_1)+F^d(\rho_2-\rho_1)}{w_1} = \frac{E+\rho_2 F^d}{w_1} - \rho_1\frac{E+\rho_2 F^d}{w_1} \quad (3)$$

$$\frac{dp_2}{dt} = \frac{F^u(\rho_1-\rho_2)}{w_2} = \frac{w_1+w_2}{w_1+w_2}\rho F^u - \rho_2\left(\frac{w_1+w_2}{w_1+w_2}F^u\right) \quad (4)$$

The subscripts 1 and 2 indicate the lower and upper layers, respectively. Vertical integration is performed from 50 hPa to 700 hPa for the upper layer and from 700 hPa to 1000 hPa for the lower layer.

To simulate the moisture sources and budgets with 2L-DRM, it is utilized hourly precipitation and evapotranspiration data from ECMWF Reanalysis v5 (ERA5), as known for its realistic estimates of hydrological variables. Additionally, its 3-hourly

horizontal wind and specific humidity data from 25 vertical levels are extracted, along with vertical velocity at 700 hPa. To examine synoptic-scale atmospheric and land changes during flood events, we also retrieved 500 and 850 hPa geopotential height and surface soil moisture data. The dataset spans a 41-year period, from 1 January 1980 to 31 December 2020. To optimize computational efficiency, the raw data were re-gridded to a 75 km horizontal resolution.

2.3 Statistical Analyses

2.3.1 Empirical Orthogonal Functions (EOF)

EOF analysis, on the other hand, is a powerful method for uncovering dominant patterns within large datasets (Yue et al., 2020). By decomposing spatiotemporal data into orthogonal basis functions, this method isolates key patterns and their associated temporal variations (Wang et al., 2017). The process involves: (1) Normalization: to standard data to have zero mean and unit variance; Covariance Matrix: to calculate the covariance matrix of the normalized data; (2) Eigenvalue Decomposition: to determine the eigenvalues and eigenvectors of the covariance matrix; (3) EOF Modes and Principal Components identify the spatial patterns (EOF modes) represented by the eigenvectors and the temporal variability (principal components). We applied EOF analysis to the anomaly fields for annual, summer, and winter periods.

2.3.2. Maximum Lag Correlation

To investigate the relationship between the TAV and ENSO index and the precipitable water resulting from 2L-DRM, the maximum lag correlation method based on the autoregressive vector, as shown by Zita et al.(2025) is employed. This technique is useful to identify the time lag at which the correlation between two time series reaches its peak, providing insights into potential cause-and-effect relationships or delayed responses in climate systems.

The maximum lag correlation coefficient between two time series, and , is computed using cross-correlation analysis. It is defined as:

$$Lag_{Corr}(\tau) = \frac{1}{n-\tau} \cdot \sum_{k=1}^{n-\tau} \left\{ \left[\frac{x(k)-\bar{x}}{\sigma_x} \right] \cdot \left[\frac{y(k+\tau)-\bar{y}}{\sigma_y} \right] \right\} \quad (7)$$

where:

- τ is the time lag,
- x and $\bar{x}$ are the mean and standard deviation of the series, respectively,
- y and $\bar{y}$ are the mean and standard deviation of the series, respectively,
- n is the total number of observations.

2.3.3. Climate Indices

Further research is essential to understand the impact of oceanic variability on precipitation. Patterns associated with the TAV and the ENSO can affect the quantity of moisture from different sources that are precipitable in the target region. These oceanic phenomena induce anomalies in precipitation leading to changes in environmental conditions far from their origins (Schumacher et al., 2022).

2.3.3.1 Tropical Atlantic Variability (TAV)

Tropical Atlantic Variability refers to fluctuations in sea surface temperatures (SST) across the tropical Atlantic, which significantly influence climate patterns in Brazil. Negative SST anomalies in the northern tropical Atlantic are linked to increased convective activity over northern and northeastern Brazil, leading to higher precipitation and elevated soil moisture levels in these regions. Utilda et al. (2019) highlight that regional precipitation along South America's coast is not solely driven by the north-south displacement of the ITCZ in response to Northern Hemisphere climate variations. Instead, the contraction and expansion of the tropical rainbelt—regulated by SST fluctuations and southeast trade winds within the tropical South Atlantic basin—also play a crucial role. Conversely, positive SST anomalies in the southern tropical Atlantic enhance moisture convergence, increasing rainfall in southeastern and southern Brazil, which results in higher soil moisture levels in these areas (Bernardino et al., 2017).

2.3.3.2 El Nino-Southern Oscillation (ENSO)

El Niño-Southern Oscillation is a climate phenomenon characterized by periodic variations in sea surface temperatures (SST) in the central and eastern equatorial Pacific, influencing global atmospheric circulation and weather patterns (Hagen and Azevedo, 2024). ENSO has two main phases: El Niño, associated with warmer SSTs, and La Niña, linked to cooler SSTs (Builes-Jaramillo et al., 2023). In the Central-West region of Brazil, which includes the Cerrado biome, ENSO plays a crucial role in modulating precipitation. During El Niño events, atmospheric circulation changes often lead to suppressed convection and reduced rainfall, increasing the risk of droughts, particularly during the wet season (Correia Filho et al., 2021). Conversely, La Niña conditions enhance moisture transport from the Amazon and favor convective activity, generally resulting in above-average precipitation (Correia Filho et al., 2021). These fluctuations impact water availability, agriculture, and wildfire occurrence in the Cerrado, a biome highly dependent on seasonal rainfall patterns.

These climatic systems do not operate in isolation, and their interactions can produce all sorts of precipitation and soil moisture patterns. For example, the interaction between ENSO and TAV can significantly modify expected climatic impacts in certain regions (Kayano et al., 2011). Additionally, other systems such as the SACZ and cold fronts may also play important roles in modulating precipitation and soil moisture in Brazil (Bernardino et al., 2017), in association with those oceanic modes of climate variability.

2.2.4 Fire analyses

Fire Radiative Power (FRP) is a measure of the energy released by active fires in the form of thermal radiation (Saide et al., 2023). It is expressed in megawatts (MW) and provides an estimate of fire intensity at a given location and time. FRP is an important parameter for quantifying fire dynamics, including fire severity, combustion efficiency, and emissions of greenhouse gases and aerososl (Lu et al., 2022).

FRP data used in this study was derived from the MODIS Terra Active Fire Product (MOD14A1, Collection 6.1), which provides daily global fire observations at 1 km spatial resolution. The dataset includes fire detections based on the thermal infrared (IR) signature of actively burning fires, with FRP representing the rate of radiative energy release (measured in megawatts, MW). FRP values were extracted over the Center-West region of Brazil for the period 2005–2020, filtering for pixels within the study area. The MOD14A1 dataset was selected due to its long temporal record, which allows for analyzing fire trends in relation to climate variability and ENSO phases. Data processing and analysis were conducted using Google Earth Engine (GEE), where FRP values were aggregated at the regional scale to assess seasonal and interannual variations.

3 Results

3.1 Moisture Sources for the sink region

Fig. 2 presents the result of 2L-DRM in mm, this analysis highlights the origin of moisture in relation to different atmospheric layers.

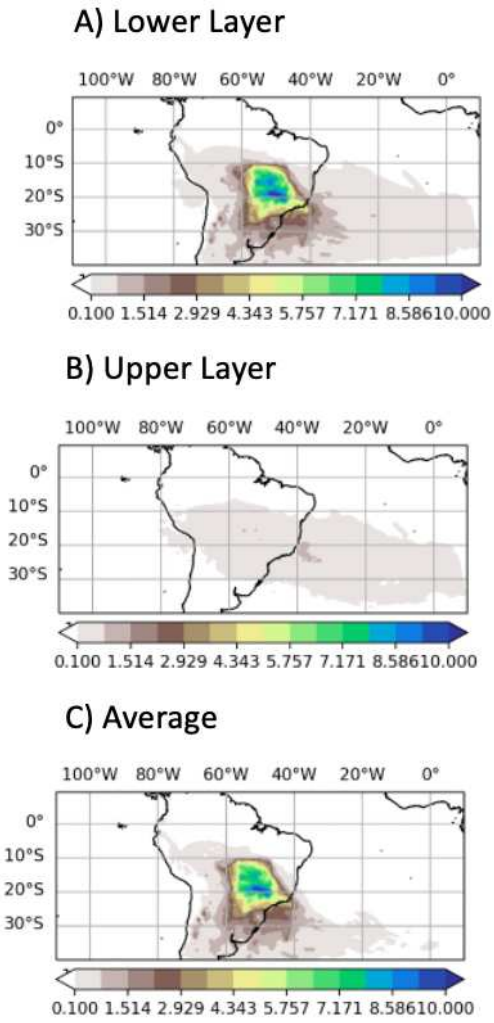

Fig. 2: Daily average precipitable water resulted from 2L-DRM (unit: mm): atmospheric layers' contributions to precipitation in the central region of Brazil, divided into the lower layer (a), upper layer (b), and their average (c)

The lower layer (Fig. a), situated closest to the surface, predominantly comprises moisture contributions from local evapotranspiration and horizontal transport from nearby regions. This layer reflects interactions between land surface processes and atmospheric moisture dynamics. The target area in central Brazil shows the highest concentration of moisture contributions, as depicted by the green-to-blue shading. This pattern suggests that surface evaporation and moisture transported from neighboring regions dominate precipitation generation in this layer.

The upper layer (Fig. b) represents mid-to-upper atmospheric regions, characterized by long-distance moisture transport via high-altitude winds. This layer captures the influence of large-scale atmospheric circulation. Moisture contributions in this layer are more diffuse and widespread compared to the lower layer. Despite their

lower intensity, these contributions play a critical role in transporting moisture from distant sources, such as the Atlantic and Pacific oceans (He et al., 2021).

The average layer (Fig. c) integrates the contributions from both the lower and upper layers, providing a comprehensive view of the atmospheric moisture supply for precipitation in central Brazil. The spatial distribution in this panel closely mirrors the lower layer, indicating the dominant role of near-surface processes. However, the average also captures the broader-scale dynamics influenced by the upper layer.

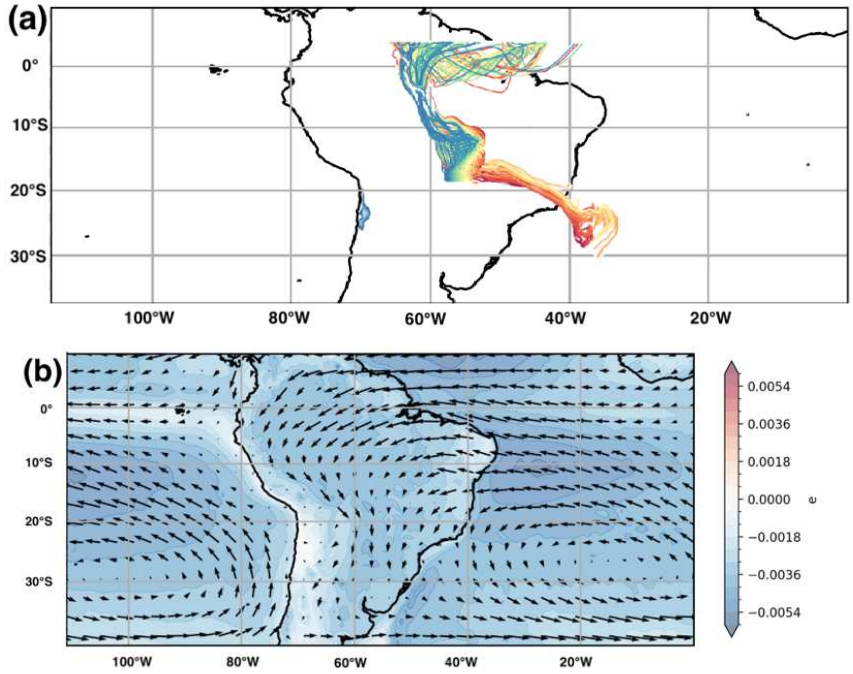

Fig.3: Moisture flux trajectories (a) and wind field and vertical velocity (ω) at 850 hPa over South America (b).

The analysis of moisture flux trajectories (Fig.3a) and large-scale wind circulation (Fig.3b) provides insights into the transport mechanisms responsible for precipitation in the Cerrado. The back-trajectory analysis (Fig.3a) reveals that moisture reaching the central-western region of Brazil primarily originates from two key sources: (i) the Amazon Basin, where intense evapotranspiration contributes to atmospheric moisture, and (ii) the tropical Atlantic Ocean, from which easterly winds transport moisture inland. Additionally, a southward extension of moisture pathways is observed, likely associated with the SACZ. The wind field analysis (Fig.3b) supports these findings, as the low-level wind patterns exhibit a predominant northeasterly flow

transporting moisture from the Atlantic Ocean into the continent. Over the Amazon, these winds converge with southerly inflows, reinforcing the moisture advection toward central Brazil as seen by Custodio et al., 2017.

Furthermore, the southeastern extension of the moisture flux trajectories corresponds well with the wind circulation over southern Brazil, where the SACZ is known to play a crucial role in moisture convergence. The alignment between the moisture transport pathways and wind field dynamics reinforces the robustness of the trajectory computations and highlights the dominant mechanisms governing seasonal precipitation variability in the region. These findings underscore the Amazon-Cerrado-Atlantic moisture connection, emphasizing the interplay between large-scale atmospheric circulation and regional precipitation patterns in South America.

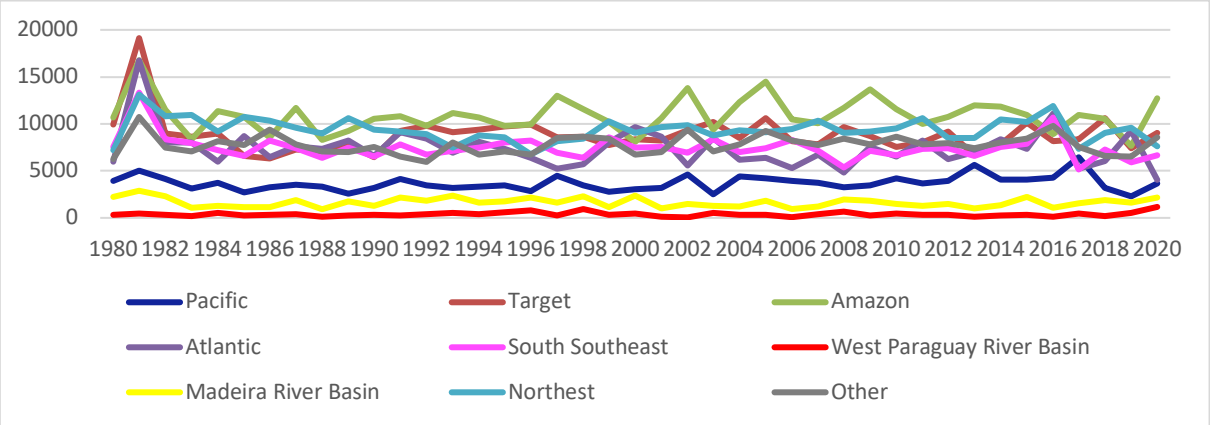

Fig.4: Monthly-Daily averaged distribution of the total precipitable water contribution from each region. X-axis shows the days 1 January to 31 December; Y-axis shows the sum of precipitable water contribution in the region in mm.

Figure 4 illustrates the annual mean precipitable water flux from various contributing regions to the target area from 1980 to 2020. Over this 41-year period, the Amazon consistently stands out as the dominant source of atmospheric moisture, with average annual contributions above 12,000 mm. Its persistent high values underscore the critical role of Amazonian evapotranspiration and convective activity in sustaining the Central-West region's hydrological cycle, particularly during austral summer months.

Following the Amazon, the West Paraguay River Basin and Other regions also display considerable contributions (typically between 10,000 and 12,000 mm per year), suggesting strong regional moisture recycling and significant influence from transient atmospheric systems like the South American Low-Level Jet (SALLJ) and mid-latitude disturbances. The Target region itself and the South-Southeast exhibit similar magnitude values (~9,000–11,000 mm), reflecting the importance of local moisture recycling and mesoscale moisture convergence mechanisms.

The Northeast and Atlantic regions maintain relatively stable contributions across the entire period (~8,000–9,500 mm), with interannual fluctuations that may be linked to variability in Tropical Atlantic Sea surface temperatures (SSTs) and ITCZ positioning. The Atlantic's steadiness points to a foundational role in supplying low-level moisture, especially during the transitional MAM and SON seasons, as suggested by seasonal analyses.

Meanwhile, contributions from the Madeira River Basin (~6,000–8,000 mm) and the Pacific (~5,000–7,000 mm) are lower but persistent. The Pacific's reduced input aligns with the Andean orographic barrier and the generally lower contribution of Pacific-origin moisture to Brazil's interior. However, Pacific ENSO phases could still exert indirect influence by modulating convection patterns over the continent (e.g., through teleconnections).

Importantly, the temporal trend shows relative stability in annual moisture contributions across all regions, with no strong upward or downward trend, suggesting that while interannual variability exists—potentially influenced by phenomena such as ENSO, TAV, or SAM—the overall climatological balance of moisture sources has remained consistent during this historical period.

This reinforces the notion that the Amazon and continental interior regions, particularly the West Paraguay River Basin and South Southeast, are indispensable to the Central-West's hydroclimate. Moreover, it emphasizes the necessity of preserving vegetation cover in these areas, as moisture recycling and land-atmosphere feedback are essential components in maintaining rainfall regimes in the target region (Zemp et al., 2014; Spracklen et al., 2012).

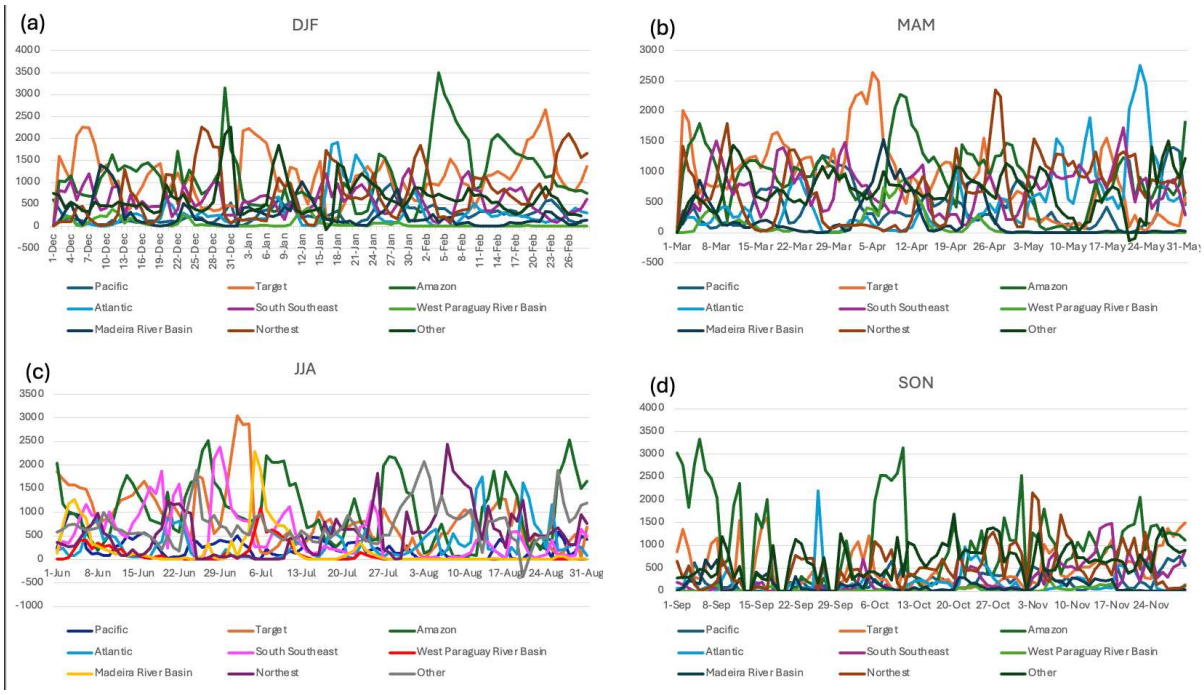

Fig.5: Seasonal-Daily averaged distribution of the total precipitable water contribution from each region. X-axis shows the days for DJF(a), MAM(b), JJA(c), and SON(d); Y-axis shows the sum of precipitable water contribution in the region in mm.

During summer (DJF) (Fig. a), moisture transport to the target region reaches its annual peak (~204,157 mm), with the Amazon acting as the leading source (~36,230 mm), followed closely by the Northeast (~34,144 mm) and the Target region itself (~30,276 mm), suggesting strong regional recycling. The West Paraguay River Basin (~27,552 mm) and Atlantic (~23,128 mm) also contribute significantly, indicating the combined effect of the South Atlantic Convergence Zone (SACZ) and Intertropical Convergence Zone (ITCZ), which intensify oceanic and continental moisture advection during this season (Chug & Dominguez, 2022; Acosta et al., 2022). Contributions from the South Southeast, Madeira River Basin, and Pacific are moderate, while Other regions (~15,322 mm) reflect transient moisture flows and recirculation, often modulated by the Tropical Atlantic Variability (TAV) (Huang & Shukla, 2005).

In autumn (MAM) (Fig. b), total moisture transport slightly decreases to ~199,842 mm, though it remains relatively high. The Atlantic Ocean now contributes the most (~31,301 mm), peaking in its seasonal role due to increased SST anomalies tied to TAV. The Amazon (~28,700 mm) and Northeast (~26,350 mm) follow, though with lower values than in DJF. The Target, South Southeast, and West Paraguay River

Basin maintain substantial contributions (~24,000–26,000 mm), which may be attributed to lingering SACZ influence and frontal systems crossing Central-West Brazil during this transition period (Luiz-Silva et al., 2020). Notably, Pacific contributions (~9,273 mm) remain minor, indicating limited influence. The Other category (~13,119 mm) continues to play a role, highlighting residual moisture advection from southern and western sources.

Winter (JJA) (Fig. c) marks the driest period (~176,503 mm), driven by the intensification of the South Atlantic Subtropical High (SASH) and the northward retreat of the ITCZ (Wong et al., 2023). During this season, moisture input from the Amazon (~25,105 mm), Target (~23,277 mm), and South Southeast (~21,450 mm) remains relevant, but reduced. The Northeast, Atlantic, and West Paraguay River Basin each contribute between ~16,000 and 19,000 mm. The Pacific reaches its lowest contribution (~7,845 mm), and the Madeira River Basin and Other regions show minimal influence, except for brief peaks associated with cold front intrusions and SALLJ events, which can still cause moisture surges from southern latitudes (Varuolo-Clarke et al., 2022).

Spring (SON) (Fig. d) reflects the transition from dry to wet seasons, with total transport increasing slightly to ~181,941 mm. The Amazon (~31,842 mm) regains influence as convection over the basin strengthens. Interestingly, the West Paraguay River Basin (~27,710 mm) and Target (~25,860 mm) exhibit robust fluxes, indicative of continental recycling and early SACZ formation. The Northeast (~24,602 mm) and Atlantic (~21,383 mm) continue to provide significant contributions, which likely increase toward the end of the season due to gradual southward ITCZ displacement and warming SSTs. The Other category (~16,305 mm) again reinforces the role of continental evapotranspiration and transient systems in supporting regional moisture availability before the onset of the rainy season (Zemp et al., 2014).

Overall, the extended analysis underscores that the Amazon remains the dominant contributor throughout the year, especially in DJF and SON. The Atlantic peaks in MAM due to favorable TAV phases, while the Northeast, West Paraguay River Basin, and Target region itself emerge as critical contributors through both local recycling and transient dynamics. The Pacific has a marginal yet consistent influence, and the Other regions, which include sources such as the La Plata Basin

and Bolivia, reveal the importance of complex cross-continental atmospheric interactions, particularly through mechanisms like SALLJ, cold fronts, and moisture recycling.

Table 1: Trends and Sen's slope estimates

	DJF	JJA	MAM	SON
Atlantic	-0.45ns	-0.52*	-0.34ns	0.79ns
Pacific	0.21ns	-0.01ns	-0.13*	1.12*
Southeast	-0.31ns	-0.32*	-0.59ns	1.67ns
Target	-0.02ns	-0.32ns	-0.005ns	1.89ns
Amazon	-0.09ns	-0.32ns	-0.22ns	1.28ns
Madeira River Basin	0.87ns	1.29ns	1.40ns	1.32ns
West Paraguay River Basin	0.04ns	0.001ns	-0.02ns	-0.001ns
Northeast	-1.87ns	0.80ns	-0.26ns	-2.15ns
Other	-0.04ns	-0.14ns	-0.31ns	0.23*
Total	0.21ns	0.55ns	0.75ns	8.76ns

ns – not significant, * Significant according to the Mann-Kendall trend test at the 95% significance level

The moisture transport trends (Table 1) reveals significant seasonal variations in the contributions of moisture from different source regions to precipitation in central South America. While most trends remain statistically non-significant at the 95% confidence level, a few significant changes indicate emerging shifts in the regional hydroclimate, particularly during the dry season (JJA) and the early wet season (SON).

During JJA, significant declines in moisture contributions are observed from the Atlantic (-0.52) and Southeast (-0.32) regions, suggesting a progressive weakening of dry-season moisture influx into the Cerrado. Although JJA is typically a period of minimal rainfall, these significant reductions may reflect an intensification of the dry season, potentially exacerbating drought conditions, increasing fire risk, and reducing water availability. In addition, a small but significant negative trend in the “Other” category (-0.14) further supports a widespread reduction in dry-season moisture transport.

In SON, while the total moisture transport shows a strong positive trend (+8.76, $p < 0.05$), it is not statistically significant, likely due to high interannual variability. However, the Pacific region exhibits a significant increasing trend (+1.12*), reinforcing the growing influence of Pacific climate variability—especially La Niña conditions—on the early onset of the rainy season. This is consistent with previous findings that link enhanced Pacific moisture transport with stronger early-season precipitation in central Brazil. A small but significant increase in the “Other” category (+0.23*) may also reflect localized shifts in atmospheric circulation or storm activity. In contrast, contributions from the Atlantic (+0.79ns), Amazon (+1.28ns), and Southeast (+1.67ns) during SON remain positive but not statistically significant, suggesting that while the Pacific influence is strengthening, traditional moisture sources show considerable variability.

The core wet season months (DJF and MAM) do not show widespread significant trends. In MAM, however, the Pacific region presents a small but significant decreasing trend (-0.13*), indicating a weakening role in late wet-season moisture delivery. All other source regions, including the Atlantic (-0.34ns), Southeast (-0.59ns), and Amazon (-0.22ns), show non-significant trends during this season. This relative stability in MAM moisture sources may conceal more subtle changes or indicate delayed responses to broader climate drivers. Similarly, DJF trends across all regions are non-significant, though the Atlantic (-0.45ns) and Southeast (-0.31ns) show weak negative values, pointing toward a possible, though statistically inconclusive, drying signal during the peak of the wet season.

Basin-specific patterns show generally weak and non-significant trends. The Madeira River Basin presents consistently positive values across all seasons (+1.40 in MAM and +1.32 in SON), though none are statistically significant, suggesting a

potentially stable or slightly increasing role in regional moisture transport. The West Paraguay River Basin shows flat trends near zero in all seasons, indicating no substantial change. The Northeast region displays a notable decreasing trend in SON (-2.15ns), although it remains statistically non-significant, warranting attention in future investigations due to its sensitivity to Atlantic SST anomalies.

In summary, these findings suggest a subtle but progressive reorganization of the hydrological cycle over the Cerrado and adjacent regions. The significant drying trends during JJA and weakening moisture supply from key regions may indicate intensifying dry season conditions. Simultaneously, the increasing Pacific contribution during SON supports the hypothesis of an earlier onset of the rainy season, even if total SON moisture transport remains statistically non-significant. These hydroclimatic shifts may have serious implications for agricultural productivity, ecosystem dynamics, and water resource management in the region, reinforcing the need for continued monitoring of moisture transport trends under changing climate conditions.

3.2 EOF Dominant Pattern (spatio-temporal variability)

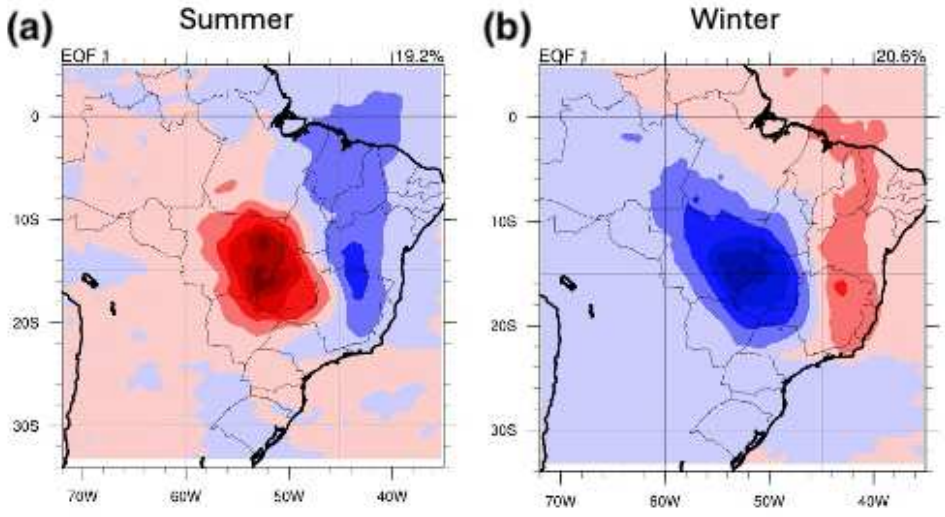

Fig. 5: First EOF Maps for Precipitable Water resulted from 2L-DRM for Summer (a) and Winter (b) Seasons over South America

The first Empirical Orthogonal Functions (EOF) for summer and winter (Fig.5a;b) in the Cerrado region reveal distinct spatial patterns that highlight the seasonal variability of atmospheric moisture in central Brazil. These patterns can be explained through the interactions of various atmospheric circulation patterns, the

SAMS, SACZ, and regional climate features, each contributing differently across the summer and winter seasons.

In the summer (Fig.5a), EOF explains a significant portion (19.2%) of the variance in precipitable water, showing a strong positive anomaly over the Cerrado region. This concentration of moisture aligns with the active phase of the SAMS, which peaks during the austral summer months (December to March). The SAMS draws moisture from the Atlantic Ocean and the Amazon Basin, creating conditions favorable for convection and heavy rainfall over central and southeastern Brazil, including the Cerrado. This monsoon system strengthens the SACZ, a band of cloud cover and precipitation extending southeastward across Brazil. The SACZ enhances the convergence of moisture over the Cerrado, resulting in the strong positive anomaly seen in EOF. The combination of SAMS and SACZ makes the Cerrado a significant moisture sink during the wet season, with high rainfall and moisture accumulation.

In winter (Fig.5b), EOF explains 20.6% of the variance and reveals a marked negative anomaly over the Cerrado region, contrasting sharply with the summer pattern. This negative anomaly signifies a lack of moisture, as the atmospheric circulation and regional climate features inhibit the transport and retention of water vapor in the area. The weakening of the SAMS and the shift in regional high-pressure systems drive this seasonal dryness.

During the winter, the SAMS weakens and retreats, effectively halting the flow of moist air masses from the Amazon and the Atlantic toward central Brazil. With the monsoon system inactive, the Cerrado receives minimal atmospheric moisture, resulting in the observed negative anomaly in EOF. This retreat of the SAMS is a primary driver of the dry season in the region. Winter in the Cerrado is characterized by the influence of the South Atlantic High, a semi-permanent high-pressure system over the Atlantic Ocean that extends its influence inland. This high-pressure area promotes atmospheric subsidence (sinking air), which suppresses cloud formation and limits precipitation over the Cerrado. This stable, dry air mass creates a barrier to moisture inflow, contributing to the negative moisture anomaly in EOF.Furthermore, unlike summer, when the SACZ enhances moisture convergence over Brazil, the SACZ is either inactive or shifts away from central Brazil in winter. This reduction in SACZ activity limits atmospheric moisture transport to the Cerrado, reinforcing the dry

season in the region. The absence of the SACZ's influence leaves the Cerrado with little external moisture, resulting in dry conditions.

3.3. Correlation between 2L-DRM results and TAV Index

The correlation map between the TAV index and precipitable water resulted from the 2L-DRM model where the sink area was defined as the Cerrado (Fig.6a) showed in Northern and Eastern Brazil (Red) positive correlations suggesting that when the TAV index is high (indicating warm anomalies in the tropical Atlantic), these regions experience an increase in precipitable water that impact the Cerrado, which could lead to wetter conditions. While Southern and Central Brazil (Blue) regions showed negative correlations here imply that an increase in the TAV index correlates with a decrease in precipitable water that impacts Cerrado, potentially causing drier conditions in these areas. As the Cerrado, located primarily in central Brazil, shows mostly negative correlations (blue shades), this suggests that an increase in the TAV index (warmer Atlantic conditions) might reduce moisture availability in this biome, impacting the regional hydrological cycle and possibly increasing drought stress.

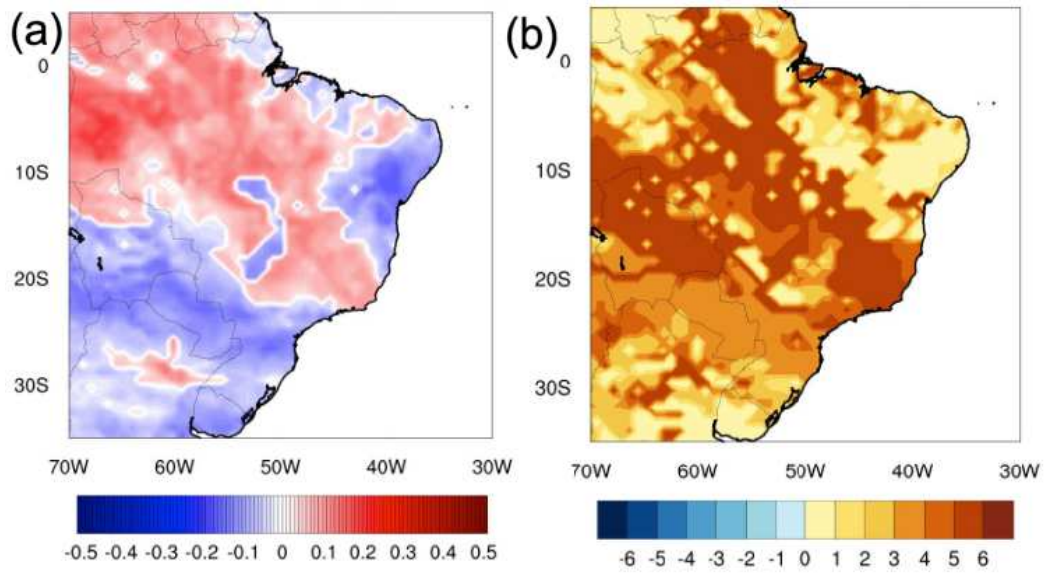

Fig. 6: Correlation (a) and Lag-Correlation (b) between TAV Index and precipitable water resulted from 2L-DRM

The map displays the lag-correlation between the TAV index and precipitable water over Brazil, with the Cerrado defined as a sink area in the 2- DRM model (Fig.6b). The positive lags in much of Brazil indicate that TAV influences precipitable water with a time delay. For water resource management and drought monitoring in the Cerrado and adjacent regions, this delayed response could be essential for anticipating seasonal shifts in moisture. As the Cerrado shows positive lag correlations (around 4 to 5 months), this implies that it is sensitive to Atlantic SST anomalies but with a delayed hydrological response, potentially affecting the region's vulnerability to seasonal droughts and consequently fires.

3.4 ENSO and TAV events

We determined the El Niño and La Niña events analyzing the Niño 3.4 Sea Surface Temperature Anomaly (SSTA) data from January 3, 1990, to January 27, 2021. The anomalies were calculated using the mean and the standard deviation (σ) of the dataset. The positive anomalies (El Niño events) were defined as SSTA values greater than 1.4°C (mean + 1.5σ), and negative anomalies (La Niña events) were defined as SSTA values less than -1.3°C (mean - 1.5σ). The highest SSTA recorded during the period was 3.1°C, while the lowest was -2.2°C. Based on these thresholds, the following periods were identified as significant El Niño or La Niña events (Table 2).

Table 2: El Nino and La Nina events from 1980-2020

Positive Anomalies (El Niño)	Negative Anomalies (La Niña)
December 4, 1991, to April 8, 1992	March 18, 1998
June 25, 1997, to March 11, 1998	July 15, 1998, to August 19, 1998
March 25, 1998	September 30, 1998, to October 21, 1998
October 23, 2002, to December 18, 2002	November 4, 1998, to February 17, 1999

January 1, 2003	August 11, 1999, to September 1, 1999
November 4, 2009, to January 13, 2010	October 27, 1999, to March 8, 2000
July 8, 2015, to March 30, 2016	October 3, 2007, to March 5, 2008
	July 28, 2010
	August 25, 2010, to February 2, 2011
	February 16, 2011, to March 2, 2011
	October 14, 2020, to November 4, 2020
	November 18, 2020, to November 25, 2020

The TAV events were determined like the El Niño and La Niña events analyzing the TAV data from January, 1980, to December, 2020. The anomalies were calculated using the mean and the standard deviation (σ) of the dataset. The positive anomalies (TAV+) were defined as values greater than 0.73°C (mean + 1.5σ), and negative anomalies (TAV-) were defined as values less than -0.73°C (mean - 1.5σ). The highest recorded during the period was 1.58°C, while the lowest was -1.18°C. Based on these thresholds, the following periods were identified as significant El Niño or La Niña events (Table 3).

Table 3: TAV- and TAV+ events from 1980-2020

TAV-	TAV+
Jun-06	Jan-05 to May-06
Jun-07 to Jul-07	Jul-06 to May-07

Sep-07	Aug-07
Dec-07	Oct-07 to Nov-07
Feb-08 to Aug-08	Jan-08
Nov-08 to Jun-09	Sep-08 to Oct-08
Dec-09 to Jan-10	Jul-09 to Nov-09
Mar-11 to Apr-11	Feb-10 to Feb-11
Jan-13	May-11 to Dec-12
Jun-13 to Jul-13	Feb-13 to May-13
Jan-14 to Aug-14	Aug-13 to Dec-13
Jan-15 to Jun-15	Sep-14 to Dec-14
Dec-15 to Apr-16	Jul-15 to Nov-15
Jun-16 to Oct-16	May-16
Dec-16	Nov-16
Mar-17 to Apr-17	Jan-17 to Feb-17
17-Oct	May-17 to Sep-17
Mar-18 to Aug-19	Nov-17 to Feb-18
Oct-19 to May-20	Sep-19
Jul-20 to Aug-20	Jun-20
	Sep-20 to Dec-20

3.5 Moisture sources during ENSO and TAV events

El Niño and La Niña events significantly influence atmospheric circulation patterns and moisture transport in South America, altering the dynamics of the SACZ and affecting the contribution of different moisture source regions to precipitation in the cerrado of Brazil. Fig.7a represents boxplots of the anomalies between the actual precipitated moisture and the daily climatic average (1980–2020) during El Niño events, while Fig.7b presents the same results for La Niña periods. The analyzed moisture sources include the Atlantic Ocean, southeastern Brazil, the Amazon, the target area, the Pacific Ocean, and other areas of South America.

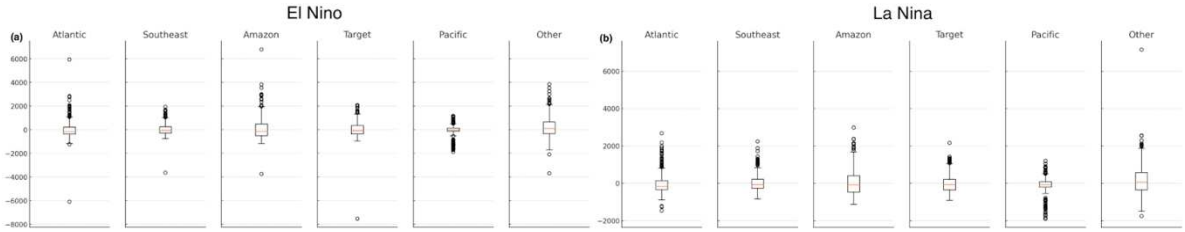

Fig. 7: Boxplots of the anomalies between the actual precipitated moisture and the daily climatic average (1980–2020) during El Niño (a) and La Niña (b)

During El Niño events, moisture flux redistribution occurs due to the weakening of the trade winds and the displacement of the Walker circulation, reducing moisture transport from the Amazon to the cerrado and potentially favoring drier conditions in the region. This pattern is evident in the boxplots, which indicate lower positive precipitation anomalies from the Amazon compared to climatology. On the other hand, there is an increase in the contribution from the Atlantic Ocean and the southeastern region, suggesting that during El Niño, moisture transported to the cerrado is influenced by anomalous SACZ patterns, with a more southward convergence and a greater influx of moisture from the tropical Atlantic.

During La Niña periods, the strengthening of the trade winds and the Walker circulation enhances moisture transport from the Amazon to the cerrado, favoring more intense precipitation events. The boxplots show an increase in positive anomalies associated with Amazonian sources, suggesting greater moisture convergence in this region. Additionally, the influence of the Pacific Ocean becomes more evident, likely associated with increased moisture flux from the tropical Pacific toward South America.

Another relevant aspect is the differentiated response of moisture originating from other areas of South America. During El Niño, these regions exhibit greater variability and more dispersed values, possibly reflecting atmospheric circulation modulation in response to anomalous Pacific warming. In La Niña, moisture anomalies from these regions tend to be more concentrated, indicating greater predictability in moisture transport.

The SACZ, which normally acts as an important moisture transport system in South America, exhibits distinct shifts in each ENSO phase. During El Niño, the SACZ weakens and shifts to more southerly latitudes, whereas in La Niña, the system intensifies and its position is closer to climatology. This behavior directly affects the variability of precipitated moisture in the cerrado, as evidenced by the presented boxplots.

The results reinforce that interannual precipitation variability in the cerrado is strongly modulated by ENSO events, affecting the relative contribution of different moisture sources to the region. Understanding these patterns is essential for seasonal forecasts and water resource management during climate extremes.

Just like ENSO, TAV modulates the SACZ and the transport of moisture from different sources to the Central-West region of Brazil. Fig.8a represents boxplots of the anomalies between the actual precipitated moisture and the daily climatic average (1980–2020) during TAV-, while Fig.8b presents the same results for TAV+ periods. The analyzed moisture sources include the Atlantic Ocean, southeastern Brazil, the Amazon, the target area, the Pacific Ocean, and other areas of South America.

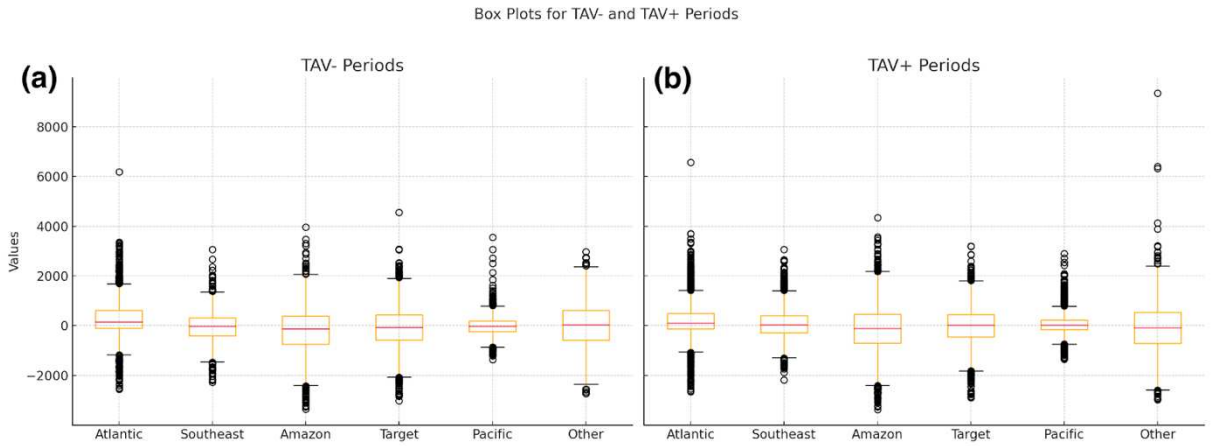

Fig. 8: Boxplots of the anomalies between the actual precipitated moisture and the daily climatic average (1980–2020) during TAV- (a) and TAV+ (b)

During TAV- periods, the thermal configuration of the Atlantic enhances trade winds, reducing convection over the tropical Atlantic and shifting the SACZ further south (Jorgetti et al., 2014). This directly influences moisture transport to the Central-West region. The contribution of moisture from the Atlantic shows high variability, with a symmetrical distribution of anomalies around the mean. This suggests that while Atlantic moisture is important, its influence on the Central-West is modulated by other atmospheric factors. The influence of Amazonian moisture also shows dispersed values, but with a tendency for lower median values, indicating a reduction in Amazonian moisture transport to the Central-West. Moisture from the Pacific shows lower variability and a negative trend, suggesting that the influence of this ocean is reduced during TAV-. Internally generated moisture (Target area) in the region is distributed close to the mean, without extreme variations. The influence of “Other” regions in South America shows high dispersion, indicating significant variability in moisture origin, which may be associated with circulation patterns modulated by TAV-.

During TAV+ periods, the warmer North Tropical Atlantic enhances convection in this region, shifting the SACZ further north and promoting greater moisture convergence over central Brazil (Jorgetti et al., 2014). A slight increase in the median anomaly of moisture from the Atlantic is observed, indicating greater moisture transport to the Central-West from this source. Amazonian moisture transport to the Central-West intensifies, with an increase in positive anomalies, suggesting that the Amazon supplies more moisture during TAV+ than during TAV-. There is a slight increase in moisture from the Pacific, but with high dispersion. This suggests that the influence of

this ocean during TAV+ may be more irregular. The target region presents more frequent positive anomalies, suggesting that internal moisture recycling within the region is more active during TAV+. In the “Other” regions in South America, the dispersion of values increases, indicating that atmospheric circulation favors a more intense moisture transport from these areas to the Central-West.

It is observed that during TAV-, there is reduced Amazonian moisture transport and greater dispersion in values from other regions, indicating less organized atmospheric patterns. During TAV+, the Amazon becomes the main moisture source, reflecting a strengthening of vapor transport mechanisms associated with the SACZ and large-scale circulation.

3.6 Fire analyses

The relationship between atmospheric moisture availability and fire activity in the Cerrado biome reveals a strong climatological control over fire dynamics. As illustrated in Figure 9, periods with reduced moisture transport to the region consistently coincide with peaks in Fire Radiative Power (FRP), suggesting that atmospheric drought conditions significantly enhance fire susceptibility. This inverse relationship indicates that lower precipitable water weakens soil moisture and vegetation hydration, creating optimal conditions for biomass combustion. Although this pattern aligns with theoretical expectations, it is important to acknowledge the role of anthropogenic ignition sources, land-use change, and regional climatological anomalies, which can also contribute to fire variability independently of moisture conditions.

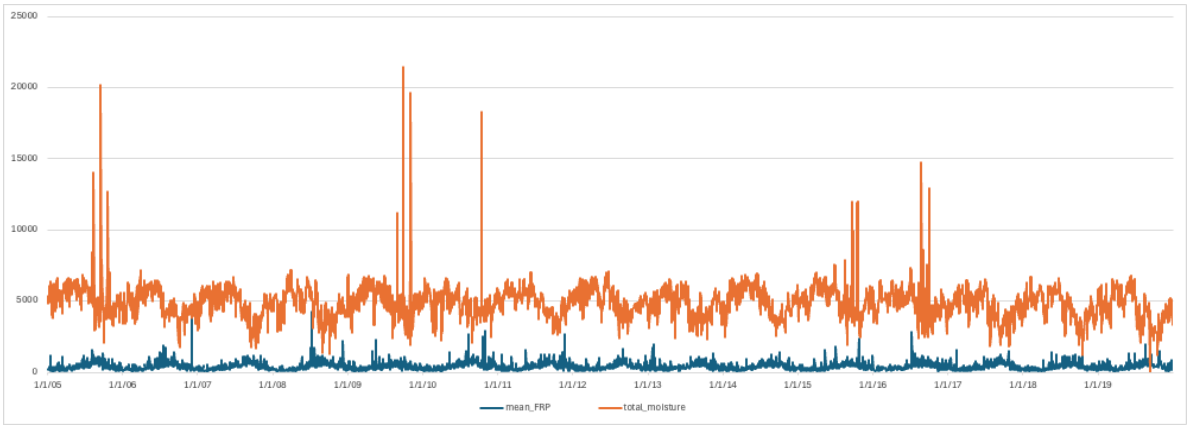

Fig. 9: FRP time series (2005-2020) and precipitable water resulted from 2L-DR

To further investigate the influence of large-scale climate anomalies on fire activity, Figure 10 overlays El Niño and La Niña periods on the FRP and Pacific moisture time series. Fire intensity follows a distinct seasonal pattern, with the majority of high-FRP events occurring during the dry season (June to October). During this period, reduced cloud cover, elevated temperatures, and increased evapotranspiration contribute to low moisture availability and dry fuels. The data reveal that El Niño phases, such as 2009–2010 and 2015–2016, are strongly associated with elevated FRP, reinforcing the well-documented suppression of precipitation by El Niño-induced subsidence and Walker circulation shifts. In contrast, La Niña events generally coincide with increased moisture availability and lower fire activity; however, exceptions like 2017–2018 highlight how regional droughts or fuel accumulation may override these favorable conditions.

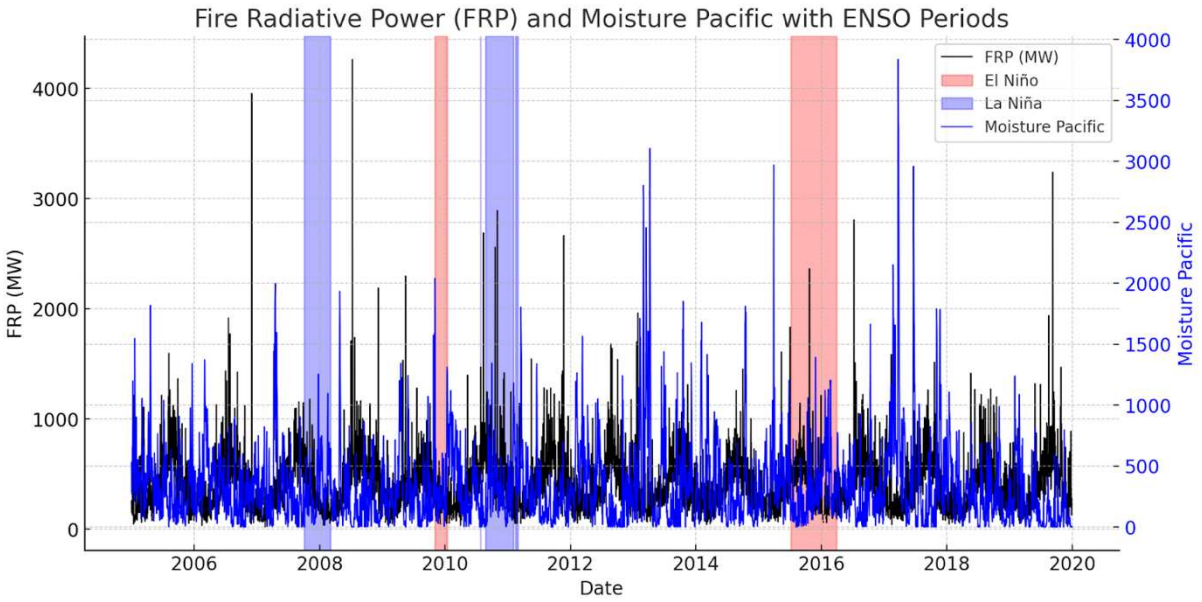

Fig. 10: FRP time series (2005-2020), precipitable water from Pacific resulted from 2L-DRM and ENSO periods highlighted

Seasonal analysis further confirms this pattern. The dry season (June–September) exhibits the highest mean FRP (~562 MW), with extreme events surpassing 4000 MW. Fire activity remains elevated into October (~512 MW) as landscapes remain dry, despite initial wet season rainfall. In contrast, the wet season (November–March) shows the lowest average FRP (~298 MW), driven by high precipitation and elevated soil moisture levels. The late wet season (April–May) also records low FRP (~301 MW), reflecting transitional conditions ahead of the next fire season. While seasonality remains the primary driver of fire dynamics, ENSO-related anomalies can intensify fire risk during already dry months or promote fuel buildup during wetter phases, increasing fire susceptibility in subsequent years.

Figure 11 illustrates the influence of Tropical Atlantic Variability (TAV) phases on FRP, with TAV+ (warm anomalies) and TAV− (cool anomalies) overlaid against Atlantic moisture flux. Overall, fire activity remains seasonally consistent; however, notable differences emerge between climate phases. TAV+ periods generally coincide with enhanced moisture availability and slightly reduced fire activity, though some years (e.g., 2015 and 2017) still show elevated FRP, likely due to compounding effects of drought or land-use change. TAV− phases, particularly 2008–2009 and 2016, often correspond with lower FRP, suggesting that cool Atlantic anomalies may support convective development and precipitation, buffering against fire spread.

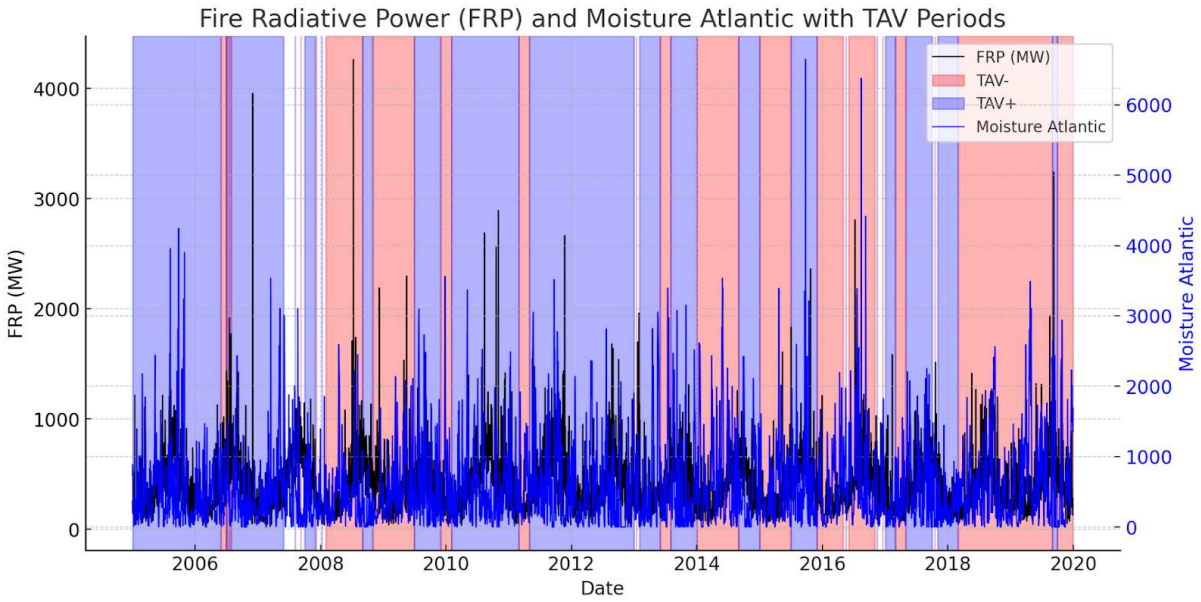

Fig. 11: FRP time series (2005-2020), precipitable water from Pacific resulted from 2L-DRM and TAV periods highlighted

To statistically validate these visual patterns, we analyzed FRP and moisture values during identified ENSO and TAV phases between 2005 and 2020. Results show that average FRP during El Niño was 334 MW, with a maximum average peak of ~1495 MW. During TAV− phases, FRP was similarly elevated (~346 MW), supporting the hypothesis that dry-phase anomalies intensify fire risk. Interestingly, La Niña events recorded the highest average FRP (~738 MW), a counterintuitive result that may be attributed to localized droughts, human ignition sources, or delayed fuel accumulation effects. In contrast, TAV+ periods showed lower FRP (~400 MW) and higher moisture availability (~4607 mm), supporting the notion that enhanced Atlantic convection offers some mitigation against fire outbreaks.

These statistical findings reinforce the idea that El Niño and TAV− periods promote fire-conducive conditions through atmospheric drying, even when mean moisture values appear relatively stable. Minimum precipitable water levels during these events were often <3500 mm, indicating brief but critical drought windows that align with fire peaks. Conversely, TAV+ conditions emerge as more consistent fire-suppressing phases, though their effectiveness depends on concurrent climate dynamics. These results underscore the importance of combining real-time climate monitoring with regional land management to improve fire forecasting and mitigation strategies in the Cerrado.

4 Conclusion

This study provides compelling evidence that moisture fluxes from the Atlantic, Pacific, and Amazon significantly influence fire activity in the Cerrado biome. By integrating the 2L-DRM model with ERA5 reanalysis data and MODIS FRP observations, we showed that large-scale climate patterns such as ENSO and TAV modulate moisture transport and fire risk. El Niño and TAV− phases consistently result in reduced moisture availability and higher FRP values, indicating drier atmospheric conditions that favor fire ignition and spread. In contrast, TAV+ phases support greater moisture transport and appear to suppress fire activity, although this relationship is modulated by local environmental factors.

EOF and lag-correlation analyses revealed strong seasonality in moisture transport, with significant reductions in austral winter contributing to fire peaks in late dry seasons. These insights are critical for fire forecasting and management, as they suggest that real-time climate monitoring and moisture anomaly tracking can serve as early indicators of upcoming fire seasons. Our findings highlight the need for integrated land-climate management strategies and stress the importance of conserving upwind moisture sources such as the Amazon Basin. Future research should incorporate high-resolution fuel load maps, human ignition data, and socio-environmental drivers to develop comprehensive fire risk models for the region.

This research provides a comprehensive analysis of the seasonal and interannual variability of atmospheric moisture fluxes into central Brazil, integrating source region contributions, trend analysis through Empirical Orthogonal Functions (EOF), and the influence of climate modes such as ENSO and TAV on fire dynamics. By applying the 2L-DRM model and decomposing moisture fluxes into directional components, we quantified the role of distinct source regions—including the Amazon, Atlantic, Pacific, Madeira River Basin, West Paraguay River Basin, Northeast Brazil, South-Southeast Brazil, and other continental areas—in modulating regional precipitation.

The results indicate that the Amazon and Atlantic remain dominant moisture contributors throughout the year, especially during the wet season. However, continental regions such as the Southeast and West Paraguay Basin also provide

critical moisture influxes, particularly in the early and late wet seasons (SON and MAM), supporting precipitation over the target region through both synoptic-scale advection and land-atmosphere recycling. Notably, contributions from the Northeast and South-Southeast persist even during the dry season, highlighting their potential to buffer against extreme drought.

Trend analysis based on EOF decomposition revealed a significant decline in total moisture transport during the core rainy season (DJF–MAM) and a moderate increase in SON, pointing to a shortening and intensification of the wet season. These seasonal shifts align with recent climate studies indicating increased variability in the South American Monsoon System. Some source regions (e.g., Pacific and Southeast) showed significant trends in their flux patterns, suggesting reorganization of large-scale circulation, possibly linked to the poleward shift of subtropical systems and altered SACZ dynamics.

The influence of ENSO and TAV was found to be critical in shaping these moisture transport patterns. El Niño conditions were associated with reduced moisture contributions from both oceanic and continental sources, weakening the SACZ and leading to drier conditions over central Brazil. La Niña phases, in contrast, enhanced the Pacific and Amazonian moisture influx, strengthening convergence zones and delaying the onset of the dry season. Positive TAV phases were related to increased Atlantic moisture transport, while TAV− phases suppressed convective development in the region. These modes modulate both the intensity and the timing of moisture delivery to the Cerrado.

Importantly, the moisture flux variability is tightly coupled to fire activity across central Brazil. Cross-correlation analyses revealed that decreases in moisture transport from key sources—particularly the Atlantic, Amazon, and South-Southeast—precede increases in fire occurrence by several weeks, indicating a strong climatic control over fire potential. The fire response is most sensitive during MAM and SON, transitional seasons in which reductions in rainfall and early drying can rapidly lead to increased fire susceptibility. These findings support the development of predictive tools that incorporate moisture source behavior, climate mode forecasts, and lagged fire response to improve early warning systems for fire risk management.

In conclusion, this work highlights the complex interplay between atmospheric moisture transport, large-scale climate variability, and fire dynamics in the Cerrado. Understanding how both oceanic and continental sources interact across timescales is essential for forecasting hydroclimatic extremes and mitigating their ecological and socioeconomic impacts. Sustained monitoring of these fluxes and their drivers is therefore critical in the face of ongoing climate change and land-use transformation in central South America.

References

Acosta, R. P., Ladant, J., Zhu, J., & Poulsen, C. J. (2022). Evolution of the Atlantic Intertropical Convergence Zone, and the South American and African monsoons over the past 95-Myr and their impact on the tropical rainforests. *Paleoceanography and Paleoclimatology*, *37*(7). https://doi.org/10.1029/2021pa004383

Arraut, J. M., Nobre, C., Barbosa, H. M., Obregon, G., & Marengo, J. (2012). Aerial rivers and lakes: looking at large-scale moisture transport and its relation to Amazonia and to subtropical rainfall in South America. *Journal of Climate*, *25*(2), 543-556.

Arruda, V.L.S., Alencar, A.A.C., de Carvalho Júnior, O.A. *et al.* Assessing four decades of fire behavior dynamics in the Cerrado biome (1985 to 2022). *fire ecol* 20, 64 (2024). https://doi.org/10.1186/s42408-024-00298-4

Chug, D., Dominguez, F., & Yang, Z. (2022). The Amazon and La Plata River Basins as moisture sources of South America: Climatology and Intraseasonal Variability. *Journal of Geophysical Research Atmospheres*, *127*(12). https://doi.org/10.1029/2021jd035455

Bernardino, B.S., Vasconcellos, F.C. and Nunes, A.M.B. (2017). Impact of the equatorial Pacific and South Atlantic SST anomalies on extremes in austral summer precipitation over Grande river basin in Southeast Brazil. *International Journal of Climatology*, 38, pp.e131–e143.

doi:https://doi.org/10.1002/joc.5358.

Builes-Jaramillo, A., Valencia, J., & Salas, H. D. (2023). The influence of the El Niño-Southern Oscillation phase transitions over the northern South America hydroclimate. *Atmospheric Research*, *290*, 106786.

Cattelan, L. G., Mattos, C. R., Pamplona, M. B., & Hirota, M. (2024). Mapping Climatic Regions of the Cerrado: General Patterns and Future Change. *International Journal of Climatology*, *44*(16), 5857-5872.

Cerri, C. E. P., Cerri, C. C., Maia, S. M. F., Cherubin, M. R., Feigl, B. J., & Lal, R. (2018). Reducing Amazon Deforestation through Agricultural Intensification in the

Cerrado for Advancing Food Security and Mitigating Climate Change. *Sustainability*, *10*(4), 989. https://doi.org/10.3390/su10040989

Correia Filho, W. L. F. C., De Oliveira-Júnior, J. F., Da Silva, C. A., Junior, & De Barros Santiago, D. (2021). Influence of the El Niño–Southern Oscillation and the sypnotic systems on the rainfall variability over the Brazilian Cerrado via Climate Hazard Group InfraRed Precipitation with Station data. *International Journal of Climatology*, *42*(6), 3308–3322. https://doi.org/10.1002/joc.7417

Custodio, M. S., Da Rocha, R. P., Ambrizzi, T., Vidale, P. L., & Demory, M. (2016). Impact of increased horizontal resolution in coupled and atmosphere-only models of the HadGEM1 family upon the climate patterns of South America. Climate Dynamics, 48(9–10), 3341–3364. https://doi.org/10.1007/s00382-016-3271-8

Dominguez, F., Hu, H., & Martinez, J. A. (2020). Two-Layer Dynamic Recycling Model (2L-DRM): Learning from Moisture Tracking Models of Different Complexity. *Journal of Hydrometeorology*, *21*(1), 3–16. https://doi.org/10.1175/jhm-d-19-0101.1

Feron, S., Cordero, R. R., Damiani, A., MacDonell, S., Pizarro, J., Goubanova, K., Valenzuela, R., Wang, C., Rester, L., & Beaulieu, A. (2024). South America is becoming warmer, drier, and more flammable. *Communications Earth & Environment*, *5*(1). https://doi.org/10.1038/s43247-024-01654-7

Ficklin, D. L., Null, S. E., Abatzoglou, J. T., Novick, K. A., & Myers, D. T. (2022). Hydrological intensification will increase the complexity of water resource management. *Earth S Future*, *10*(3). https://doi.org/10.1029/2021ef002487

Grimm, A.M. How do La Niña events disturb the summer monsoon system in Brazil?. *Climate Dynamics*22, 123–138 (2004). https://doi.org/10.1007/s00382-003-0368-7

Hagen, M. and Azevedo, A. (2024) El Niño-Southern Oscillation (ENSO) Variations and Climate Changes Worldwide. *Atmospheric and Climate Sciences*, 14, 233-249. doi: 10.4236/acs.2024.142015.

He, Z., Dai, A., & Vuille, M. (2021). The joint impacts of Atlantic and Pacific multidecadal variability on South American precipitation and temperature. *Journal of Climate*, 1–55. https://doi.org/10.1175/jcli-d-21-0081.1

Hofmann, G. S., Silva, R. C., Weber, E. J., Barbosa, A. A., Oliveira, L. F. B., Alves, R. J. V., Hasenack, H., Schossler, V., Aquino, F. E., & Cardoso, M. F. (2023). Changes in atmospheric circulation and evapotranspiration are reducing rainfall in the Brazilian Cerrado. *Scientific Reports*, *13*(1). https://doi.org/10.1038/s41598-023-38174-x

Huang, B., & Shukla, J. (2005). Ocean–Atmosphere interactions in the tropical and subtropical Atlantic Ocean. *Journal of Climate*, *18*(11), 1652–1672. https://doi.org/10.1175/jcli3368.1

Jorgetti, T., da Silva Dias, P.L. & de Freitas, E.D. The relationship between South Atlantic SST and SACZ intensity and positioning. *Clim Dyn* 42, 3077–3086 (2014). https://doi.org/10.1007/s00382-013-1998-z

Kayano, M.T., Andreoli, R.V. and de Souza, R.A.F. (2011). Evolving anomalous SST patterns leading to ENSO extremes: relations between the tropical Pacific and Atlantic Oceans and the influence on the South American rainfall. *International Journal of Climatology*, 31(8), pp.1119–1134.

doi:https://doi.org/10.1002/joc.2135.

Kim, S., & Dominguez, F. (2023). Warm season extreme flood events in the Midwestern US—Sources of moisture and physical mechanisms. *Journal of Geophysical Research: Atmospheres*, *128*(14), e2022JD038208.

Lu, X., Zhang, X., Li, F., & Cochrane, M. A. (2022). Improved estimation of fire particulate emissions using a combination of VIIRS and AHI data for Indonesia during 2015–2020. Remote Sensing of Environment, 281, 113238. https://doi.org/10.1016/j.rse.2022.113238

Luiz-Silva, W., Oscar-Júnior, A. C., Cavalcanti, I. F. A., & Treistman, F. (2020). An overview of precipitation climatology in Brazil: space-time variability of frequency and intensity associated with atmospheric systems. *Hydrological Sciences Journal*, *66*(2), 289–308. https://doi.org/10.1080/02626667.2020.1863969

Marengo, J.A., Jimenez, J.C., Espinoza, JC. *et al.* Increased climate pressure on the agricultural frontier in the Eastern Amazonia–Cerrado transition zone. *Sci Rep* 12, 457 (2022). https://doi.org/10.1038/s41598-021-04241-4

Nobre, J. P. G., Gan, M. A., Vendrasco, É. P., Ferreira, T. R., & Vieira Cavalcante, L. C. (2025). Land-atmosphere coupling over West-Central Brazil during South American monsoon rainy season: a diagnostic study using reanalysis. *Theoretical and Applied Climatology*, *156*(2), 103.

Oliveira, U., Soares-Filho, B., Bustamante, M., Gomes, L., Ometto, J. P., & Rajão, R. (2022). Determinants of fire impact in the Brazilian biomes. *Frontiers in Forests and Global Change*, *5*. https://doi.org/10.3389/ffgc.2022.735017

Pereira Júnior, A. C., Oliveira, S. L. J., Pereira, J. M. C., & Turkman, M. a. A. (2014). Modelling fire frequency in a Cerrado Savanna protected area. *PLoS ONE*, *9*(7), e102380. https://doi.org/10.1371/journal.pone.0102380

Pivello, V. R., Vieira, I., Christianini, A. V., Ribeiro, D. B., Da Silva Menezes, L., Berlinck, C. N., Melo, F. P., Marengo, J. A., Tornquist, C. G., Tomas, W. M., & Overbeck, G. E. (2021). Understanding Brazil's catastrophic fires: Causes, consequences and policy needed to prevent future tragedies. *Perspectives in Ecology and Conservation*, *19*(3), 233–255. https://doi.org/10.1016/j.pecon.2021.06.005

Ribeiro, A.F.S., Santos, L., Randerson, J.T. *et al.* The time since land-use transition drives changes in fire activity in the Amazon-Cerrado region. *Commun Earth Environ* 5, 96 (2024). https://doi.org/10.1038/s43247-024-01248-3

Rodrigues, A. A., Macedo, M. N., Silvério, D. V., Maracahipes, L., Coe, M. T., Brando, P. M., Shimbo, J. Z., Rajão, R., Soares-Filho, B., & Bustamante, M. M. C. (2022). Cerrado deforestation threatens regional climate and water availability for agriculture and ecosystems. *Global Change Biology*, *28*(22), 6807–6822. https://doi.org/10.1111/gcb.16386

Saide, P. E., Krishna, M., Ye, X., Thapa, L. H., Turney, F., Howes, C., & Schmidt, C. C. (2023). Estimating fire radiative power using weather radar products for wildfires. *Geophysical Research Letters*, *50*(21). https://doi.org/10.1029/2023gl104824

Schumacher, V., Justino, F., Leonardo, N.F. *et al.* Disentangling the role of the Pacific and Atlantic Oceans during the Amazonian droughts in 2015. *Theor Appl Climatol* 148, 1057–1067 (2022). https://doi.org/10.1007/s00704-022-03998-6

Schmidt, I. B., & Eloy, L. (2020). Fire regime in the Brazilian Savanna: Recent changes, policy and management. *Flora*, *268*, 151613. https://doi.org/10.1016/j.flora.2020.151613

Senande-Rivera, M., Insua-Costa, D., & Miguez-Macho, G. (2025). Climate change aggravated wildfire behaviour in the Iberian Peninsula in recent years. *Npj Climate and Atmospheric Science*, *8*(1). https://doi.org/10.1038/s41612-025-00906-3

Silva, V. B., & Kousky, V. E. (2012). The South American monsoon system: Climatology and variability. Modern climatology, 123, 152.

Utida, G., Cruz, F.W., Etourneau, J., Bouloubassi, I., Schefuß, E., Vuille, M., Novello, V.F., Prado, L.F., Sifeddine, A., Klein, V., Zular, A., Viana, J.C.C. and Turcq, B. (2019). Tropical South Atlantic influence on Northeastern Brazil precipitation and ITCZ displacement during the past 2300 years. *Scientific Reports*, 9(1). doi:https://doi.org/10.1038/s41598-018-38003-6.

Varuolo-Clarke, A. M., Williams, A. P., Smerdon, J. E., Ting, M., & Bishop, D. A. (2022). Influence of the South American Low-Level Jet on the Austral Summer precipitation trend in southeastern South America. *Geophysical Research Letters*, *49*(9). https://doi.org/10.1029/2021gl096409

Wang, T., Franz, T.E., Li, R., You, J., Shulski, M.D. and Ray, C. (2017). Evaluating climate and soil effects on regional soil moisture spatial variability using EOFs. Water Resources Research, 53(5), pp.4022–4035.

doi:https://doi.org/10.1002/2017wr020642.

Wong, M. L., Battisti, D. S., Liu, X., Ding, Q., & Wang, X. (2023). A North–South Dipole Response of the South Atlantic Convergence Zone During the Mid-Holocene. *Geophysical Research Letters*, *50*(23), e2023GL105130.

Yue, W., Meng, K., Hou, K., Zuo, R., Zhang, B.-T. and Wang, G. (2020). Evaluating climate and irrigation effects on spatiotemporal variabilities of regional groundwater in an arid area using EOFs. *The Science of The Total Environment*, 709, pp.136147–136147. doi:https://doi.org/10.1016/j.scitotenv.2019.136147.

Zemp, D. C., Schleussner, C.-F., Barbosa, H. M. J., van der Ent, R. J., Donges, J. F., Heinke, J., Sampaio, G., and Rammig, A.: On the importance of cascading moisture recycling in South America, Atmos. Chem. Phys., 14, 13337–13359, https://doi.org/10.5194/acp-14-13337-2014, 2014.

Zita, L. E., Justino, F., Gurjão, C., Adamu, J., & Talacuece, M. (2025). Spatio-Temporal Characteristics of Climate Extremes in Sub-Saharan Africa and Potential Impact of Oceanic Teleconnections. Atmosphere, 16(1), 86. https://doi.org/10.3390/atmos16010086

2. Conclusão Geral

Esta tese apresenta uma análise abrangente das dinâmicas interconectadas do transporte atmosférico de umidade, da variabilidade da umidade do solo e da ocorrência de incêndios na América do Sul, com foco específico no Cerrado, no período de 1980 a 2020. Ao integrar uma abordagem com múltiplos conjuntos de dados e métodos estatísticos avançados, esta pesquisa forneceu percepções críticas sobre como os grandes forçantes climáticos modulam os processos hidrológicos regionais e a suscetibilidade ao fogo.

O primeiro estudo estabeleceu que a umidade do solo na América do Sul apresenta significativa variabilidade sazonal e interanual, fortemente governada por forçantes climáticos como o ENOS e a TAV. Por meio de uma análise com múltiplos conjuntos de dados, foi revelado que, embora haja concordância geral quanto aos padrões amplos de variabilidade, existem diferenças importantes na representação de tendências e de características em escala regional, especialmente em áreas com vegetação densa, como a Amazônia. Os resultados ressaltam o papel vital da umidade do solo na regulação do ciclo hidrológico e destacam a necessidade de uma abordagem multidataset para capturar toda a complexidade das dinâmicas da umidade do solo.

O segundo estudo ampliou esses achados ao demonstrar uma ligação clara entre fluxos atmosféricos de umidade e atividade de fogo. Utilizando o modelo 2L-DRM, foi mostrado que o transporte de umidade proveniente do Atlântico, do Pacífico e da Amazônia constitui um dos principais controles sobre o risco de incêndio no Cerrado. Especificamente, as fases de El Niño e TAV− enfraquecem consistentemente o transporte de umidade, resultando em condições atmosféricas e superficiais mais secas que aumentam a probabilidade e a intensidade de surtos de fogo. Em contrapartida, as fases de La Niña e TAV+ intensificam os fluxos de umidade e reduzem a atividade de fogo. Os resultados ressaltam a importância crítica das regiões-fonte de umidade e das teleconexões climáticas de grande escala para a dinâmica regional dos incêndios.

De forma coletiva, este trabalho oferece um arcabouço para compreender e prever os desafios ambientais enfrentados pelo Cerrado. Ele evidencia que a integridade de ecossistemas distantes, em especial a Bacia Amazônica, está diretamente ligada ao equilíbrio hidrológico e à resiliência ao fogo do Brasil central. Os achados possuem implicações significativas para estratégias de adaptação climática, reforçando a necessidade de políticas que promovam a conservação das fontes de umidade a montante e a implementação de práticas sustentáveis de uso da terra.

Pesquisas futuras devem se basear nesta fundação, incorporando dados de alta resolução sobre carga de combustível, fontes antrópicas de ignição e condicionantes socioambientais. Isso possibilitaria o desenvolvimento de modelos de risco de incêndio mais abrangentes e preditivos. Além disso, uma investigação mais aprofundada sobre as discrepâncias entre modelos quanto às tendências da umidade do solo e suas bases físicas seria valiosa para aprimorar a confiabilidade das projeções climáticas e do gerenciamento de recursos hídricos diante da intensificação das mudanças climáticas. A integração desses elementos será crucial para o desenvolvimento de estratégias robustas, baseadas em dados, para proteger o Cerrado e outros ecossistemas vulneráveis contra as crescentes ameaças de eventos hidrológicos extremos e incêndios florestais.